A Study of the Magnetic Properties of Yb4LiGe4: Unusual Magnetism

Author: Jacob N. Svensson

A Study of the Magnetic Properties of Yb_4LiGe_4

Unusual Magnetism

J. Niclas Svensson

Senior Thesis

Physics Department

College of Arts and Sciences

Boston College

May 7, 2010

Table of Contents

Acknowledgements

I would like to thank everyone who has helped me with completing this thesis. Most especially, I would like to thank my advisor, Professor Michael Graf. For four years, he has been a teacher in and out of the classroom, and has especially pushed me in my growth as my research advisor for two and a half years. He has given me tremendous opportunities, experience, knowledge, and wisdom, for which I am very thankful.

Additionally, Ryan Johnson was a great help by patiently steering me in the right direction in the lab. Steve Disseler and Karen Chen were always willing to lend me a hand and help with explanations, so thanks to them as well.

Thank you also to Father Cyril Opeil, who added to my laboratory experience and was always nice enough to let me borrow equipment to make my experiments go better.

Svet Simidjiyski deserves much of my thanks as well. He always took time out of his day to help me get my experiments going and to lend a word of encouragement.

Thanks to Sean Giblin for guiding us through the μSR techniques, as well as to ISIS Rutherford Appleton Laboratory for the use of their facilities. Thanks to the National Science Foundation and the American Physics Society for their generous grants as well.

I would also like to thank Professor Graf for allowing me to play my guitar in the lab while waiting on experiments, and thank him for his own musical contributions.

Graf Lab, Spring 2010

Introduction

In this thesis, I will conduct a systematic study of the compound Yb_4LiGe_4. This synthetic compound has roots in a family of substances known as R_5T_4 compounds. However, the substitution of lithium - which is normally not associated with R_5T_4 compounds - into this material leads to some unusual magnetic properties.

This thesis will begin by going over a background of the basic physics behind magnetism. Then, it will describe R_5T_4 compounds in general, and the parent compound, Yb_5Ge_4, in specific. Subsequently, the compound Yb_4MgGe_4 will be discussed because of its similarity to Yb_4LiGe_4.

After that, the results of earlier experiments on Yb_4LiGe_4, such as magnetization, specific heat, and susceptibility measurements will be discussed. Then, recent results from μSR studies as well as resistance measurements of the material under pressure will be reported. Finally, a discussion of conclusions will transpire.

Magnetism

Basically, magnetism arises due to the motion of electric charge. According to the classical Biot – Savart Law:

$$\mathbf{B}(\mathbf{r}) = \frac{\mu_0}{4\pi}\int \frac{\mathbf{I}\times\hat{\mathbf{r}}}{r^2}\,dl'$$

where the integration is performed over a current path and μ_0 is the permeability of free space, $\mu_0 = 4\pi \times 10^{-7}$ N/A^2, combined with the Right Hand Rule for straight-line currents, one finds that current loops form magnetic dipoles. Analogously, in quantum mechanics, the motion of charges results in magnetic moments. Thus, the magnetic moment of an electron stems from its total angular momentum, J, where J is the sum of the orbital angular momentum, L, and the spin angular momentum, S. Then, since materials are made up of lots of atoms full of

electrons, magnetism is bound to show up. Of course, the magnetic dipoles usually point in random directions, which leads to a net magnetic field of zero. However, the dipole moments can be aligned by applying an external field, resulting in a polarization that is either parallel or anti-parallel to the applied field. These results are called paramagnetism and diamagnetism, respectively. For this thesis, only paramagnetism is relevant, so diamagnetism will not be discussed.[1]

Paramagnetism

Keeping in mind the idea of a magnetic dipole as a current loop, one finds that the torque on a dipole is:

$$\boldsymbol{\tau} = \mathbf{m} \times \mathbf{B}$$

where **m** is the magnetic dipole moment of the loop (pointing in the direction of the current) and **B** is the applied magnetic field. Thus, one would expect that all magnetic dipoles, and consequently all ions, would align parallel to an applied field. In a ground state configuration where the orbital angular momentum is zero, though, sometimes the opposite spins of the electrons in an ion lead to a total spin, and hence total angular momentum, of zero. Then there would be no magnetic moment and thus no torque or paramagnetism.

For certain numbers of electrons, the total spin cannot be zero. This is very significant. Consider, for example, the two ionization states for the ytterbium ion: Yb^{3+} and Yb^{2+}. According to Hund's Rules, which come from quantum mechanics, the Pauli Exclusion Principle, and model calculations, the electrons in a ground state configuration will maximize the total spin and then maximize the total angular momentum that is consistent with the total spin.[2]

Thus, we have the ground state electronic configurations of Yb^{3+} and Yb^{2+}:

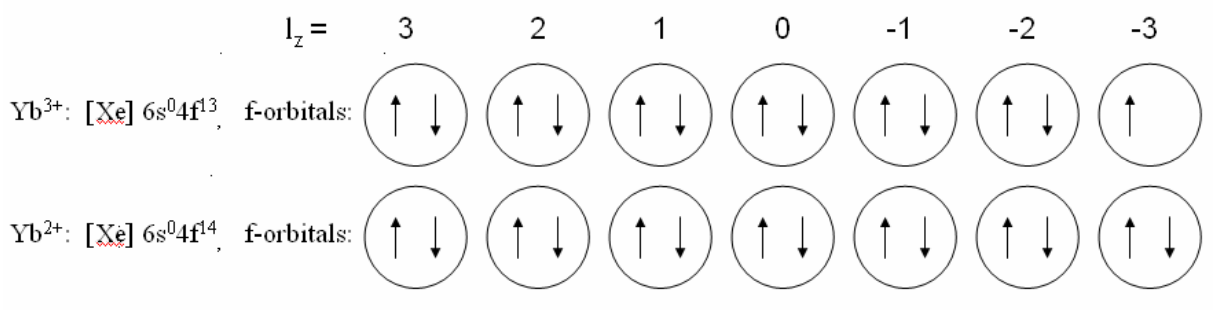

Figure 1: Ground State Configurations of Yb^{3+} and Yb^{2+}.

Here, it is obvious that Yb^{3+} is magnetic, while Yb^{2+} is not. The difference of one electron changes the ion's magnetic properties.

Curie Law

One magnetic property that all paramagnets share is their positive magnetic susceptibility. In fact, that is how one defines a paramagnet. To understand susceptibility, first magnetization must be defined. Magnetization is the magnetic dipole moment per volume of the material,

$$M = \frac{Nm}{V}$$

where N is the number of dipole moments and m is their strength. Then, susceptibility is defined as the magnetization per applied magnetic field:

$$\chi = \frac{M}{H} = \frac{\mu_0 M}{B}$$

Therefore, to say that paramagnets have magnetic moments that tend to align along the field direction means that they have positive susceptibilities.

If statistical mechanics is used to find the average magnetization, an interesting result for susceptibility is found. First off, the energy levels for an electron in a magnetic field are

$$E = -\vec{\mu} \cdot \vec{B} = m_J g \mu_B B$$

Where μ is the effective magnetic moment, g is the spectroscopic splitting factor (g = 2 for electrons), and μ_B is the Bohr magneton defined as $\mu_B = e\hbar/2m$ for the electron charge e and mass m. Also, m_J is the projection quantum number. For an electron with no orbital moment m_J = +/- ½, so E = +/- μB. Then from statistical mechanics, the number of electrons in the positive m_J state is $N_{+1/2} = \frac{Ne^{\frac{\mu B}{k_B T}}}{e^{\frac{\mu B}{k_B T}} + e^{\frac{-\mu B}{k_B T}}}$ and the number in the negative m_J state is

$N_{-1/2} = \frac{Ne^{\frac{-\mu B}{k_B T}}}{e^{\frac{\mu B}{k_B T}} + e^{\frac{-\mu B}{k_B T}}}$. So if $\langle M \rangle = (N_{+1/2} - N_{-1/2})\mu$, the result is:

$$\langle M \rangle = \frac{N\mu e^{\frac{\mu B}{k_B T}} - N\mu e^{\frac{-\mu B}{k_B T}}}{e^{\frac{\mu B}{k_B T}} + e^{\frac{-\mu B}{k_B T}}}$$

Now, let $x = \mu B / k_B T$, so:

$$\langle M \rangle = N\mu \cdot \frac{e^x - e^{-x}}{e^x + e^{-x}} = N\mu \tanh(x)$$

For x << 1,

$$M \cong N\mu \frac{\mu B}{k_B T}$$

This results in a susceptibility of

$$\chi = \frac{\mu_0 M}{B} = \frac{N\mu_0\mu^2}{k_B T} = \frac{C}{T}$$

This is the Curie Law for paramagnets named after Pierre Curie who developed the theory, where C is the Curie constant ($C = \frac{N\mu_0\mu^2}{k_B}$). So for paramagnets, the susceptibility is inversely proportional to the temperature. This law is altered slightly for paramagnets that have interactions between individual ions: ferromagnets and antiferromagnets.

Ferromagnetism

A ferromagnet is a material with a spontaneous magnetic moment. In other words, ferromagnets can be magnetized without the help of an applied field. Strong interatomic forces in ferromagnets compel the atoms' magnetic moments to align parallel to each other. Of course, high enough temperatures force the magnetic moments to be agitated enough to break their alignment. The temperature at which ferromagnetic ordering is disrupted is called the Curie Temperature, T_c; at temperatures above T_c, the material acts like a paramagnet but with an altered form of the Curie Law.[2]

Curie-Weiss Law

If it is assumed that the moments align because of a field that is proportional to the magnetization, $B_E = \lambda M$, then starting with the paramagnetic susceptibility, χ_P, one finds:

$$\chi_P = \frac{C}{T} = \frac{\mu_0 M}{B_{total}} = \frac{\mu_0 M}{(B_{applied} + B_E)} = \frac{\mu_0 M}{(B_{applied} + \lambda M)}$$

$$\Rightarrow \quad C(B_{applied} + \lambda M) = CB_{applied} + C\lambda M = \mu_0 MT$$

$$\Rightarrow \quad CB_{applied} = \mu_0 M\left(T - \frac{\lambda C}{\mu_0}\right)$$

$$\Rightarrow \quad \frac{\mu_0 M}{B_{applied}} = \frac{C}{\left(T - \frac{\lambda C}{\mu_0}\right)}$$

$$\Rightarrow \quad \chi(T) = \frac{C}{(T - T_c)} \qquad \text{where } T_c = \frac{\lambda C}{\mu_0}$$

This result is called the Curie-Weiss Law named for Pierre Curie and Pierre Weiss who developed the theory. The Curie-Weiss Law is obviously only applicable to temperatures above T_c. One sees that at $T = T_c$, the susceptibility diverges to infinity. Physically, this calls attention to the fact that ferromagnets can have magnetization with zero applied magnetic field. Thus, if a compound has a Curie Temperature, it strongly indicates ferromagnetism. There is another strong indicator for ferromagnetism other than a T_c, though.

Hysteresis

Having a T_c is definitely characteristic of ferromagnets, but some physicists argue that hysteresis is an even more distinctive sign.[3] Hysteresis is observed by measuring the magnetization of a sample while a magnetic field is applied, then slowly reversed, and then slowly reversed again back to the initial field. One would think that for the same values of magnetic field, the sample would have the same magnetization. If hysteresis occurs, though, this is not the case. A typical hysteresis loop would look like the following figure:

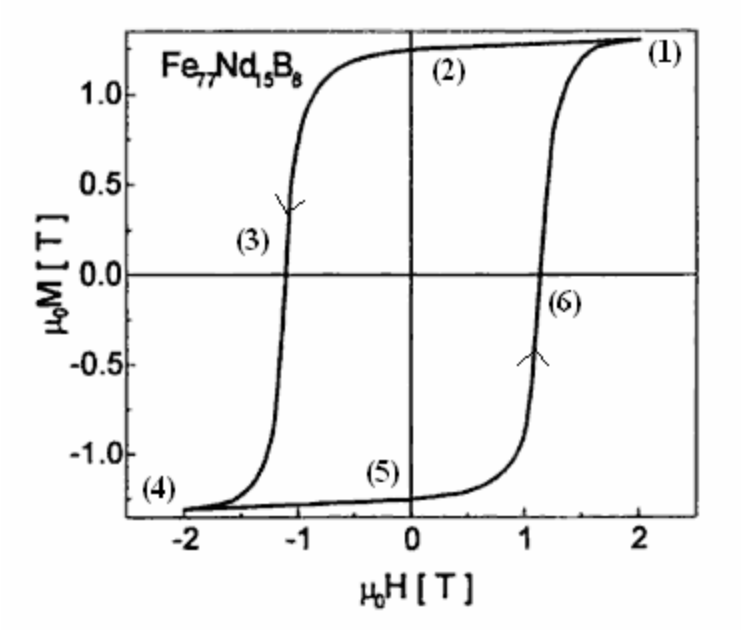

Figure 2: Hystesis for $Fe_{77}Nd_{15}B_8$. [3]

Here, the magnetization is different depending on whether the field strength is increasing or decreasing.

What is the cause of hysteresis? Well, if a strong enough magnetic field is applied, all of the moments in a ferromagnet will align with that field (area (1) in the figure). But, as mentioned above, if the field is reduced to zero, there will still be a net magnetization; the moments want to stay aligned with each other, (2). When one begins to apply a magnetic field in the opposite direction, though, the moments will eventually start to align with that, (3). Then, when the magnetic field is decreased once again, the same effect as before occurs; the moments want to stay aligned until they are forced to change directions, (5, 6). This is hysteresis. Hysteresis is a characteristic of ferromagnetism but not of its counterpart, antiferromagnetism.

Antiferromagnetism

Spontaneous magnetization is not confined to parallel alignment of magnetic moments. There can also be anti-parallel alignment. In some compounds, called antiferromagnets, the individual magnetic moments tend to line up in a direction opposite their neighbors. This leads to a cancellation of the net moment. Again, there is a temperature above which the thermal agitation is dominant over the tendencies of alignment. This temperature for antiferromagnets is called the Néel Temperature, T_N, after Louis Néel who predicted antiferromagnetism in the 1930's.

Susceptibility for Antiferromagnets

The susceptibility for antiferromagnets at $T > T_N$ is similar to the Curie-Weiss Law. If one starts with the assumption that there are two spin lattices, A and B, that want to align opposite each other, and $B_A = -\mu M_B$, $B_B = \mu M_A$, then, following the earlier discussion, one finds:

$$M_A T = C(B_{applied} - \mu M_B), \quad M_B T = C(B_{applied} - \mu M_A)$$

$$\Rightarrow \quad \begin{pmatrix} T & \mu C \\ \mu C & T \end{pmatrix} = C \cdot \begin{pmatrix} B_{applied} \\ B_{applied} \end{pmatrix}$$

So, in order to find the Néel Temperature, one sets $B_{applied} = 0$ and notes that the determinant of the above matrix must equal zero in order to have nonzero solutions, implying that $T_N = \mu C$. Then, solving for M_A and M_B:

$$M_A = \frac{1}{T}\left[CB_{applied} - \frac{2\mu C B_{applied}(T - T_N)}{T^2 - T_N{}^2} \right] \qquad M_B = \frac{CB_{applied}(T - T_N)}{T^2 - T_N{}^2}$$

This results in a susceptibility for $T > T_N$ of:

$$\chi = \mu_0 \frac{M_A + M_B}{B_{applied}} = \mu \frac{2CT - 2CT_N}{T^2 - T_N{}^2}$$

$$\Rightarrow \qquad \chi(T) = \mu_0 \frac{2C}{T + T_N}$$

Right away, it is obvious that the susceptibility diverges to infinity when $T \rightarrow -T_N$, compared to the positive T_c. Thus, susceptibility offers one method of distinguishing ferromagnets and antiferromagnets experimentally. In experiment, however, the form of the susceptibility for antiferromagnets is:

$$\chi(T) = \mu_0 \frac{2C}{T + \theta}$$

and values for θ / T_N are oftentimes not unity, but for common antiferromagnets range from close to 1 up to 5.5. The differences are attributed to next-nearest neighbor interactions and different arrangements of the spin lattices.[2] In any case, whether the singularity for susceptibility occurs for a positive or a negative value of T is a good indicator of ferromagnetism or antiferromagnetism, respectively. However, it is not always black and white.

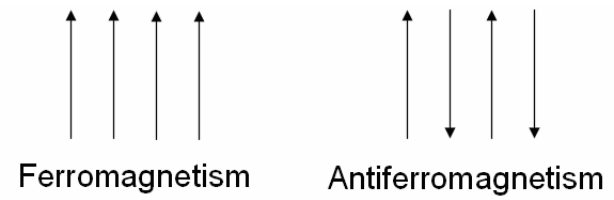

Figure 3a: In Ferromagnetism, the magnetic moments align, but in Antiferromagnetism, they align anti-parallel.

Ferrimagnetism

Sometimes some of the magnetic moments in a crystal align parallel to each other and some anti-parallel, but the two moments are not equal. This leads to somewhat of a reduced

ferromagnetism, and it is called ferrimagnetism. The anti-parallel alignment of some of the moments may be caused by differences in the chemistry of the ions or because of different local environments.[4] Some possible arrangements of magnetic moments resulting in ferrimagnetism are shown below.

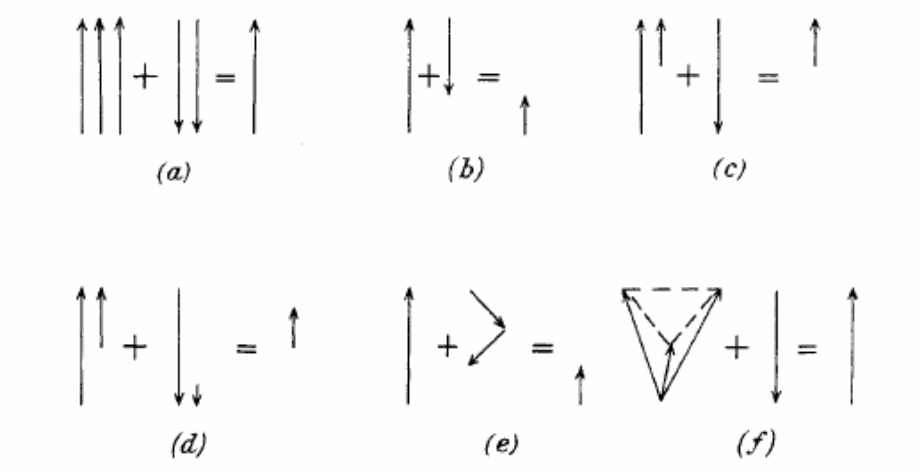

Figure 3b: Possible Orientations of Magnetic Moments for a Ferrimagnet.[4]

The susceptibility for a ferrimagnet takes the form of: $\chi = \frac{(C_A + C_B)T - 2\mu C_A C_B}{T^2 - T_C{}^2}$.

This equation is arrived at in a similar fashion as the antiferromagnetic derivation, but with two different Curie constants, C_A and C_B, representing different strengths of the magnetic moments in different lattices.

There are, of course, other forms of magnetism than paramagnetism (with ferromagnetism, antiferromagnetism, and ferrimagnetism), such as diamagnetism, but they will not be discussed because they do not pertain to the rest of this paper.

Introduction to the Compound

Now that the fundamentals of magnetism have been established, it is time to introduce the compound whose magnetic properties will be investigated in this thesis. The compound's

chemical formula is Yb_4LiGe_4. Its parent compound is Yb_5Ge_4, and it is important to classify this parent compound in order to understand what makes Yb_4LiGe_4 interesting.

R_5T_4 Compounds

Yb_5Ge_4 is an R_5T_4 compound, where R stands for Rare Earth Metals and T stands for Tetrel elements, like germanium and silicon. The R_5T_4 family of compounds was discovered in 1966, and within a year, twenty-five such compounds' structural properties had been characterized as well as some magnetic properties. One interesting find was that the Curie Temperature of gadolinium was increased by about 40 K by bonding it with non-magnetic silicon in Gd_5Si_4. Notwithstanding, there was not much interest in the compounds until 1997, when the giant magnetocaloric effect was discovered in some R_5T_4 alloys containing gadolinium.[5] This discovery gained interest because the giant magnetocaloric effect is useful for magnetic refrigeration; the effect cools refrigerators because the compound exhibiting the effect draws energy (from heat) away from the refrigerator in order to randomize its magnetic moments.[6]

From 1997 to the present, research on this family has expanded tremendously. In addition to the giant magnetocaloric effect, giant magnetoresistance was reported in R_5T_4 compounds, which is when the compound's resistivity can be lowered by applying a magnetic field.[5] This effect is used commonly in hard disk drives.

Furthermore, R_5T_4 compounds are of interest because they are very sensitive to changes in their chemistry (such as substitution or doping), and they are sensitive to temperature, pressure, and magnetic field.[5]

Yb_5Ge_4

Yb_5Ge_4 is especially interesting among R_5T_4 compounds because of the ytterbium ions that are present. As was mentioned earlier, ytterbium has two ionization states: Yb^{3+}, which is magnetic, and Yb^{2+}, which is not. Besides their magnetic properties, the two ions also differ in size; Yb^{3+} has a radius of 1.740 Å, and Yb^{2+} has a radius of 1.940 Å.[7] The two different valencies of ytterbium ions have been shown to lead to unusual behavior with regards to magnetic properties.[8] This is sometimes a result of intermediate valency, where the collection of ions acts as if all of the ions had a single valency that was a number between their integer values. Non-integral valencies can occur only when the energies of the outermost, f, electrons are almost degenerate, which is the case for ytterbium.[9]

Using Mössbauer spectroscopy, which works by shooting gamma rays (high-frequency photons) at samples and measuring the intensity of the transmitted beam in order to find out chemical properties, researchers have shown that the ratio of Yb^{3+} to Yb^{2+} ions in Yb_5Ge_4 is roughly one-to-one, and temperature-independent.[7] In other words, Yb_5Ge_4 is mixed valent, with about fifty percent of the ytterbium ions being trivalent (3+) and fifty percent being divalent (2+); and these

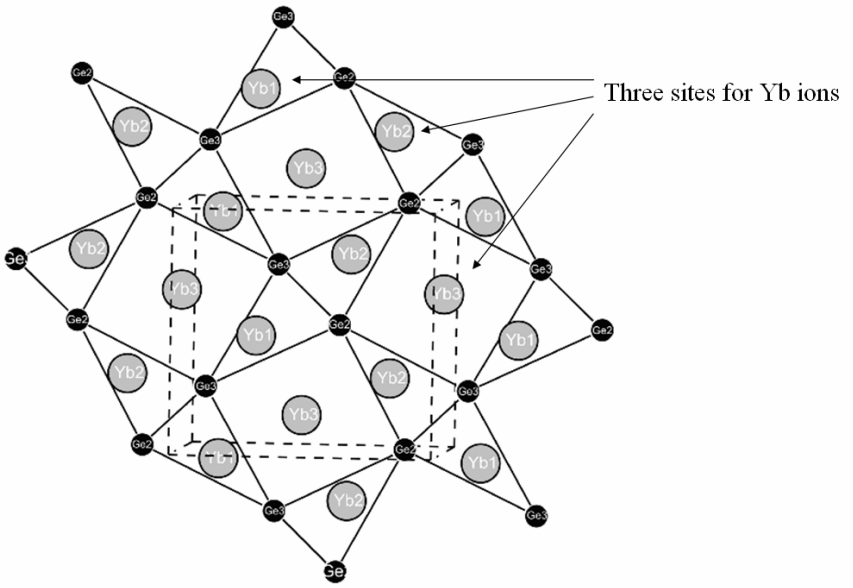

Figure 4: Crystal Structure of Yb_5Ge_4.[8]

percentages do not change with changing temperature. This ratio is even more intriguing when one considers the shape of the compound's crystal.

Researchers performed x-ray powder diffraction on samples of Yb_5Ge_4 in order to obtain information about the crystal structure. Basically, these experiments are performed by targeting a sample with a beam of x-rays, which makes elastic collisions with the atoms, and then creates a diffraction pattern. From this pattern characterized by peaks in intensity, the researchers use the method of Rietveld refinements to evaluate the lattice parameters of the crystal. The result for Yb_5Ge_4 is that it has a Gd_5Si_4-type crystal structure, which is characterized by three sites in the lattice where the ytterbium ions reside.[10]

So how do two different valencies fit evenly into three sites? That question is not so easy to answer. According to further Mössbauer spectroscopy data, the best conclusion is that it is not possible to say whether or not the different ytterbium ions have preferred sites in the lattice.[7] It is only known that the different ions exist in equal amounts.

Another idea proposed is that the ionizations of the ions fluctuate between the two states during a period of time called the valence fluctuation time. Then, one must be careful to run experiments that measure on a time-scale less than the valence fluctuation time in order to see the different ionizations states.[9]

Magnetization

In addition to the crystallographic and chemical results that have been mentioned so far, some experiments have also revealed magnetic properties. Magnetization measurements were performed on a Yb_5Ge_4 sample that was cooled with zero applied magnetic field and then warmed in a field of B = .05 Tesla, and another time with B = 5 Tesla, by Ahn et al. The results are shown in Figure 5.

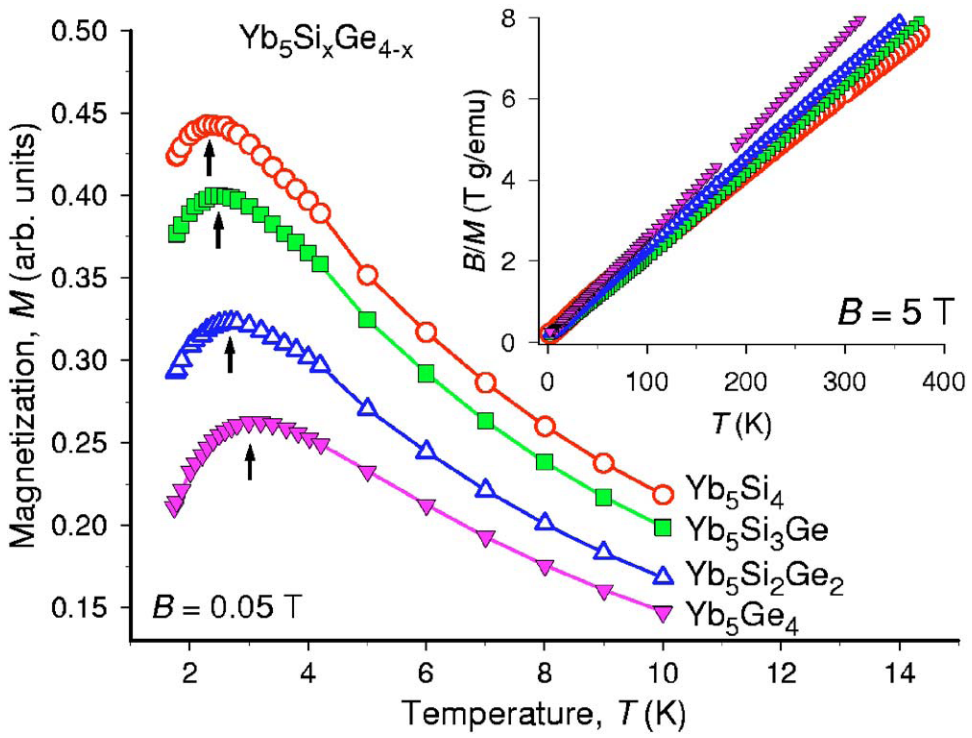

Figure 5: Magnetization of $Yb_5Si_xGe_{4-x}$.[10]

The inset is easy to interpret from the earlier discussion of susceptibility. From the Curie-Weiss Law:

$$\chi \propto \frac{M}{B} \propto \frac{1}{T - T^*} \qquad \Rightarrow \qquad \frac{B}{M} \propto \left(T - T^*\right)$$

where T* will be positive for ferromagnets and negative for antiferromagnets. Thus, in the plots in the inset of Figure 5, T* will take on the sign (positive or negative) of the intercept of the temperature axis (horizontal axis). The data for Yb_5Ge_4 followed the Curie-Weiss Law, and the intercept was negative, implying possible antiferromagnetism. Also, one can calculate from the Curie constant an effective magnetic moment of 2.1 +/- 0.2 μ_B / Yb.[10]

To interpret the results of the main part of the figure, recall that as the temperature of a paramagnet is lowered to its ordering temperature, the magnetization rises proportionally to 1/T (from the Curie-Weiss Law). However, after the critical temperature, ferromagnets will

retain a high magnetization, but antiferromagnets will have a decreasing magnetization as the magnetic moments tend to cancel each other. Thus, Figure 5 indicates antiferromagnetic ordering that occurs where there is a maximum in the magnetization curve, i.e. 3.2 K for Yb_5Ge_4. It turns out that this value for T_N is close, but not exactly the ordering temperature.

Hyperfine Fields

Once again, Mössbauer spectroscopy experiments provide valuable results. Using spectroscopic methods, Voyer et al. were able to obtain values for the hyperfine magnetic field that exists in atoms due to the interaction of electron spin and electron orbital angular momentum. Their results are shown in Figure 6.

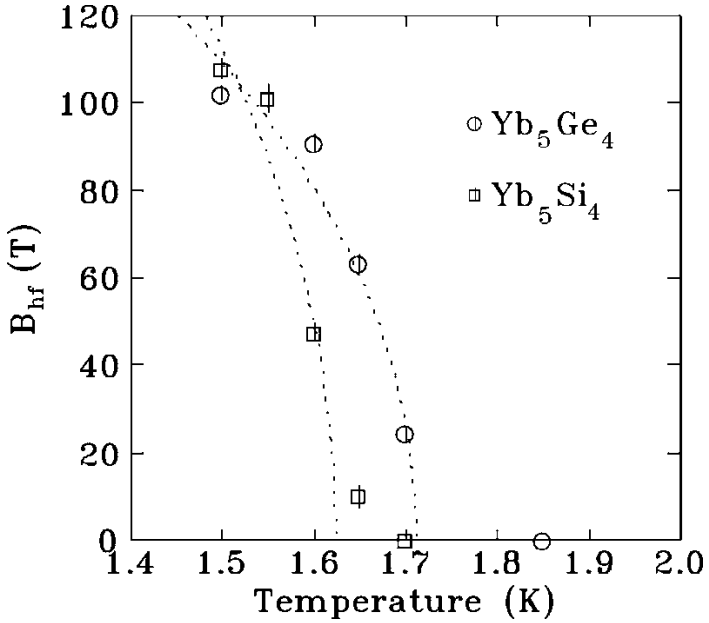

Figure 6: Hyperfine Fields of Yb_5Ge_4 and Yb_5Si_4.[7]

The dotted-line fits come from a modified version of the Curie-Weiss Law for hyperfine fields, B_{hf},

$$B_{hf}(T) = B_{hf}(0)\left(1-\frac{T}{T_N}\right)^{\beta}$$

One sees from this equation that $B_{hf} \rightarrow 0$ as $T \rightarrow T_N$. Thus, Mössbauer spectroscopy yields a Néel Temperature of 1.7 K, which is lower than the previously reported 3.2 K. The difference in the two values might be explainable by the fact that oftentimes magnetization data for R_5Ge_4 compounds performed above the ordering temperature feature anomalies that may be linked to magnetic clustering.[7] Further confirmation of a presumed antiferromagnetic transition at a temperature below 2 K comes from isothermal magnetization measurements.

Isothermal Magnetization Measurements

Performed at constant temperatures of 1.8 K and 10 K, which are both above the ordering temperature, the magnetization of Yb_5Ge_4 was measured while varying the applied magnetic field from 0 to 7 Tesla. The large increase in the magnetization for the small change in field around $B_{critical} = 1.3$ T is metamagnetic-like behavior.[10] This behavior can stem from several different causes. One possible cause is an antiferromagnetic transition. Conceptually, if there is antiferromagnetic ordering, then the magnetic moments want to be aligned anti-parallel, so they will resist lining up with the applied field. However, when the applied field increases past a critical value, the energy associated with the field will overpower the antiferromagnetism and induce many of the magnetic moments to suddenly point in the direction of the applied field. This sudden increase in magnetization can be most easily seen by the dM/dB plot in the inset Figure 7. Note that the temperature for the inset is 1.8 K, which is above $T_N = 1.7$ K. Even though it is above the ordering temperature, these results indicate the onset of ordering. Furthermore, there is no evidence of hysteresis in these measurements, which make a stronger case for antiferromagnetic ordering.

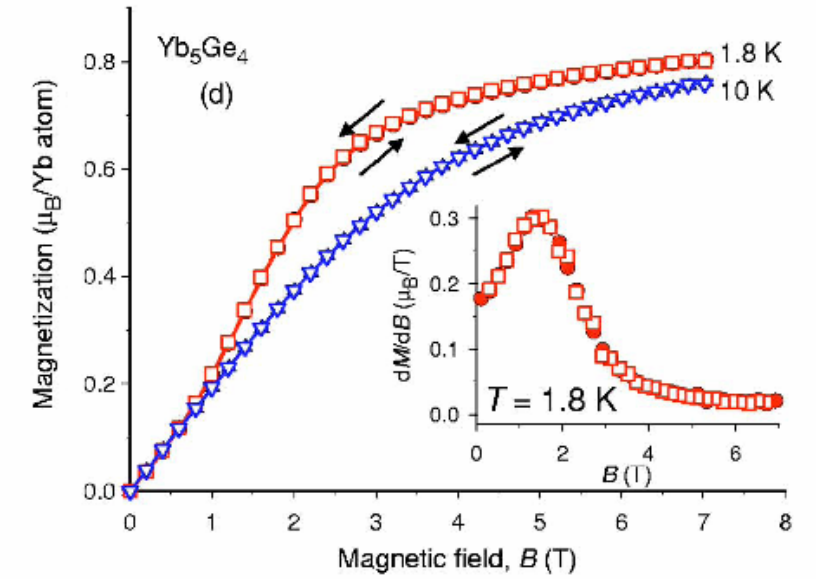

Figure 7: Magnetization as a Function of Magnetic Field.[10]

Specific Heat of Yb_5Ge_4

One last measurement that was performed on Yb_5Ge_4 was for specific heat. Specific heat is a measure of how much thermal energy (heat) is needed to raise the temperature of a quantity of a sample by one degree. Figure 8 shows the data that was obtained. The curve for Lu_5Ge_4 is included for comparison because it is non-magnetic. As one can see, the Lu_5Ge_4 curve tends toward zero as temperature approaches zero, but the Yb_5Ge_4 curves start to turn up below 9 K. This is a sign of the magnetism inherent in Yb_5Ge_4. Additionally, the fact that

the upturn exists until the magnetic field applied to the system is raised substantially above $B_{critical}$ points once again to antiferromagnetic tendencies.

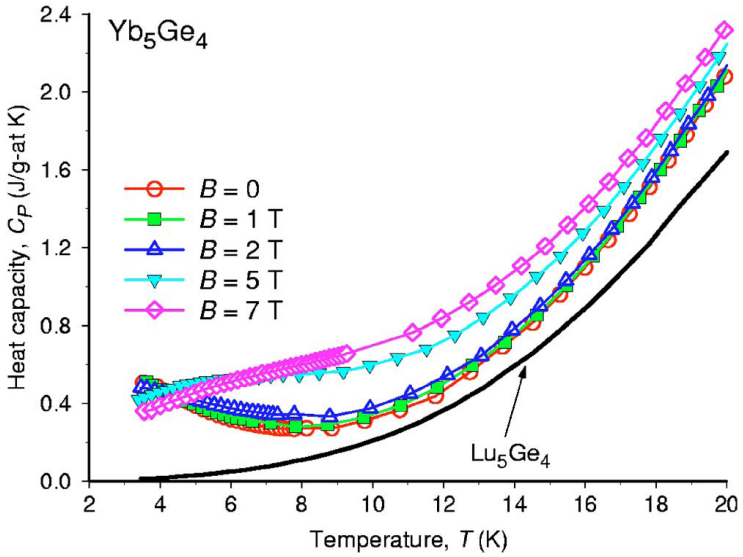

Figure 8: Heat Capacity of Yb_5Ge_4.[10]

Thus, through several experiments utilizing several different techniques, Yb_5Ge_4 has qualified itself as an appealing compound to study. It has an interesting crystallographic structure, two different ionization states of ytterbium present, and strong indications of antiferromagnetic ordering at 1.7 K. These are all good signs that substituting a lithium ion for one of the ytterbium ions might have some exciting effects.

Substitutions

Many of the properties of the parent compound, Yb_5Ge_4, have been characterized and discussed above, so why would it interesting to try to do the same for Yb_4LiGe_4? In the past several years, there has been a number studies of variations of Yb_5Ge_4. These mostly involved the substitution of silicon for germanium in the form $Yb_5Si_xGe_{4-x}$, which was an obvious choice since silicon and germanium are the two most common T – elements in R_5T_4 compounds. It turns out that for most R_5T_4 compounds (except R = Yb) for which there is experimental data, the silicides (R_5Si_4 compounds) share one crystal structure, while the

germanides (R_5Ge_4 compounds) share a crystal structure that is different from the silicides' one. Also, other than R = Yb, the silicides in this family are ferromagnetic but the germanides are antiferromagnetic. However, the studies of $Yb_5Si_xGe_{4-x}$ demonstrated that both Yb_5Si_4 and Yb_5Ge_4 share the same crystal structure and are both antiferromagnetic.[10] So, already, Yb_5Ge_4 sets itself off as an outlier from the rest of the R_5T_4 family when it comes to substitutions.

Then, if substitutions of the T – element in Yb_5Ge_4 have atypical outcomes, what will happen when substituting for the R – element? In various studies, the R – element has been replaced with other R – elements, causing differences in structure and chemical properties.[11] Now, it has already been discussed that compounds containing ytterbium have unusual traits, so replacing ytterbium ions with other ions should definitely result in noticeable differences. This is especially true when one recalls that there are two types of ytterbium present in Yb_5Ge_4, one that is magnetic and one that is not. So one question that is immediately at hand is: Which ionization state will be affected by the substitution?

Yb_4MgGe_4

One team of researchers that has taken up the objective of answering this question is headed by Paul Tobash and Svilen Bobev of the University of Delaware. They studied the compound Yb_4MgGe_4 using susceptibility measurements, with the results as shown in Figure 9. Note that in this case, ytterbium is being substituted by

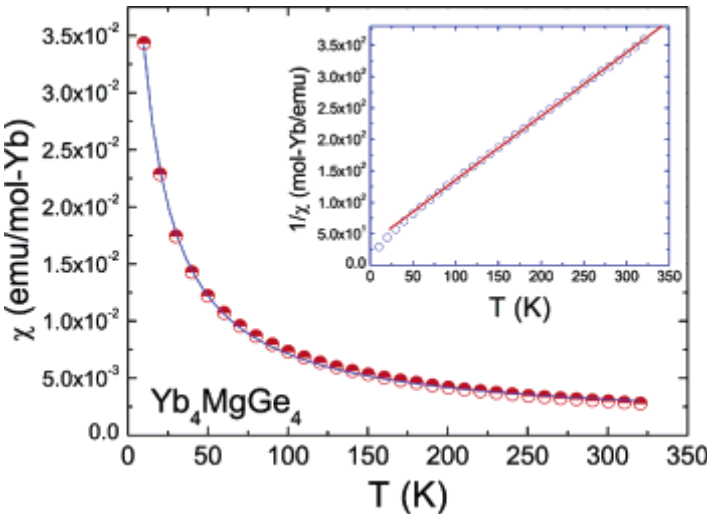

Figure 9: Susceptibility of Yb_4MgGe_4.[11]

a non-magnetic ion, Mg^{2+}. The susceptibility follows a modified Curie-Weiss Law of the form: $\chi(T) = \chi_0 + \frac{C}{(T - T^*)}$, where χ_o is the sum of temperature-independent contributions to the susceptibility. Then, the effective magnetic moments can be extracted from the Curie constant. For Yb_4MgGe_4, the effective magnetic moment was found to be 2.3 μ_B / Yb, which indicates that the ratio of ytterbium ions is still almost one-to-one.[11]

A similar experiment was run using $Yb_{3.76}Mg_{1.24}Ge_4$, which yielded an effective moment of 2.2 μ_B / Yb, leading to a ratio for Yb^{3+} : Yb^{2+} of .9 : 1.[11] The lower effective moment implies that the addition of Mg^{2+} ions displaces more of the magnetic Yb^{3+} ions than the non-magnetic Yb^{2+}. This result may be due to the fact that non-magnetic Mg^{2+} has an ionic radius that is closer in size to Yb^{3+} ions.[11]

The fit of the susceptibility data to the modified Curie-Weiss Law also yielded a T* value of -11 K.[11] This negative value implies possible antiferromagnetism, and it is consistent with the parent compound.

The results of the Yb_4MgGe_4 experiments imply that substituting a non-magnetic lithium ion for one of the ytterbium ions will also lead to some interesting results. Thus, Yb_4LiGe_4 calls for a comprehensive investigation, utilizing several different experimental techniques.

<u>Yb_4LiGe_4</u>

Using x-ray spectroscopy, the orthorhombic primitive cell of Yb_4LiGe_4 was seen to have lattice parameters of: a = 7.0828 Å, b = 14.6415 Å, c =

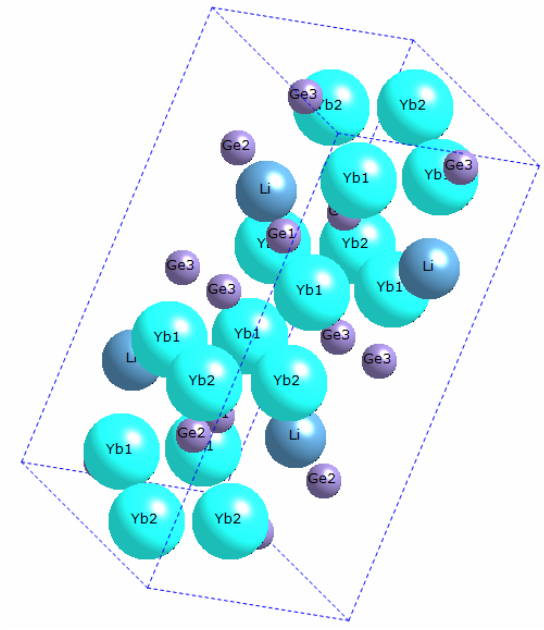

Figure 10: Crystal Structure of Yb_4LiGe_4.[21]

7.6279 Å. These are the dimensions of the primitive cell of the compound. Yb_4LiGe_4 has the Sm_5Ge_4 type crystal structure. Further, the substitution of the lithium ion for an ytterbium ion distorts the shape of the arrangement of germanium ions slightly, which may be responsible for some changes in properties.[8]

Data regarding the valency of the ytterbium ions came from x-ray absorption spectroscopy (XAS). The absorptions for different photon beam energies can be seen in Figure 11. The peak at 8948 eV is related to the Yb^{3+} ions, and the peak at 8941 eV is from the Yb^{2+} ions. The result is a derived valence state of 2.57, as in $Yb^{2.57+}$.[8]

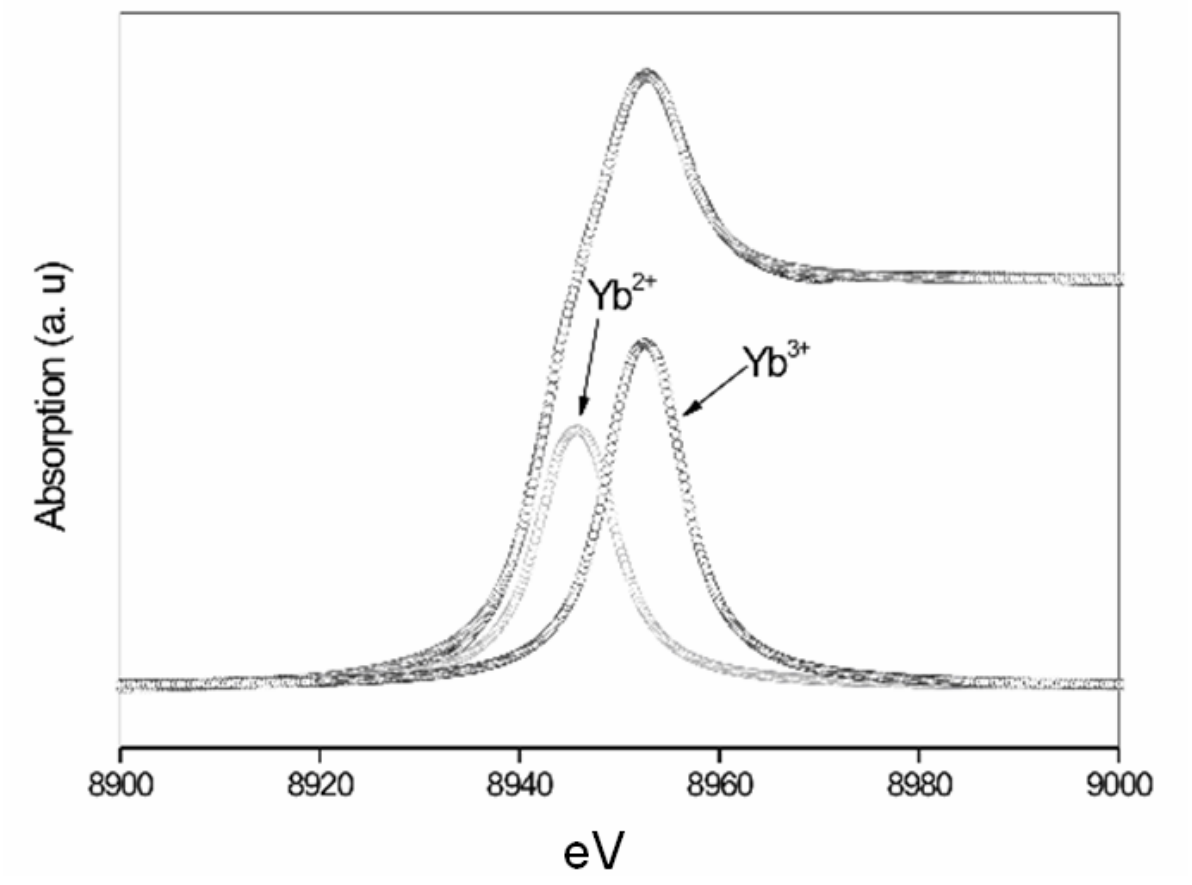

Figure 11: Absorptions for the Two Ytterbium Ions.[8]

Previous Measurements

Now that some of the crystallographic and ionic properties of Yb_4LiGe_4 have been presented, the next order of business is to look at what experiments have been performed on the compound that comment on its magnetic properties.

Magnetization

Magnetization measurements were performed on a sample of Yb_4LiGe_4 using a SQUID magnetometer at a temperature of 1.8 K. The results are shown in Figure 12. What was evident in the Yb_5Ge_4 data does not show up for Yb_4LiGe_4. That is, the magnetization increases with a smooth curve instead of experiencing any sudden and dramatic increases. This is clear from the inset of dM/dB.

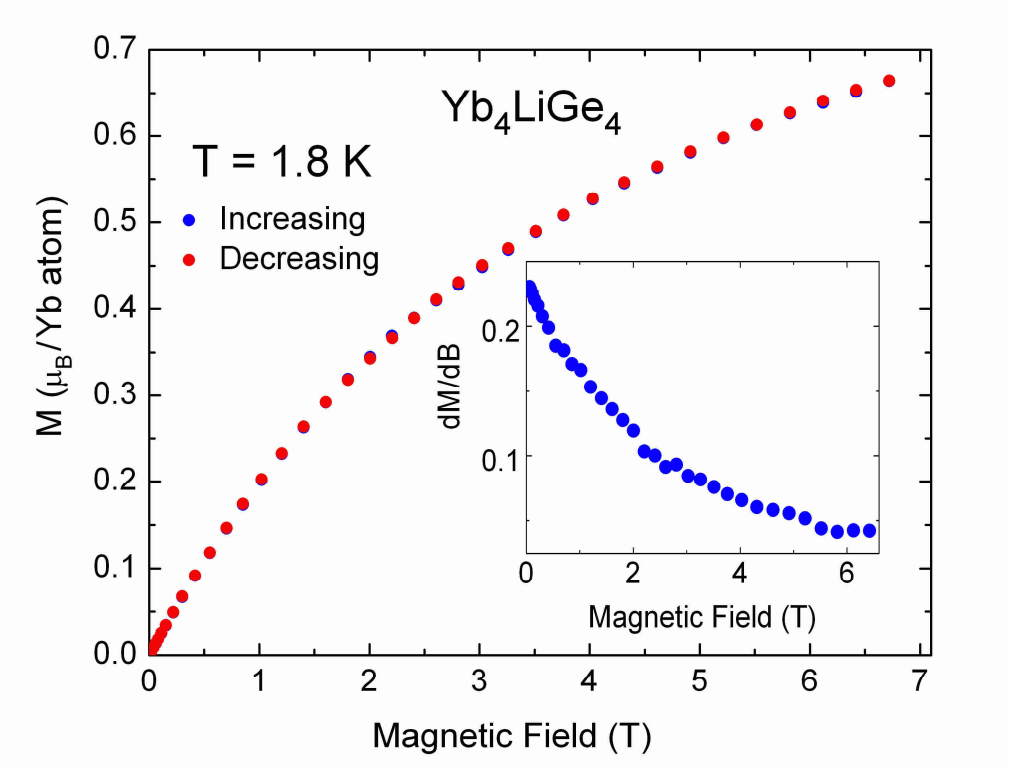

Figure 12: Magnetization of Yb_4LiGe_4.[8]

Thus, one sees that the substitution of the lithium ion has definitely played a role in changing the magnetic properties of Yb_4LiGe_4 from those of the parent compound. Recall, though, that the Néel Temperature of the parent compound is 1.7 K, which is below the temperature at which these measurements took place. Hence, the absence of a signature of magnetic ordering does not preclude the possibility of magnetic ordering. This magnetization data implies that more experiments must be performed to gain greater clarity.

Specific Heat

Specific heat measurements were performed on a Yb_4LiGe_4 sample at temperatures ranging from 3 to 60 K. Looking at the results in Figure 13 and comparing them to those of the parent compound, one can see that they are quite similar.

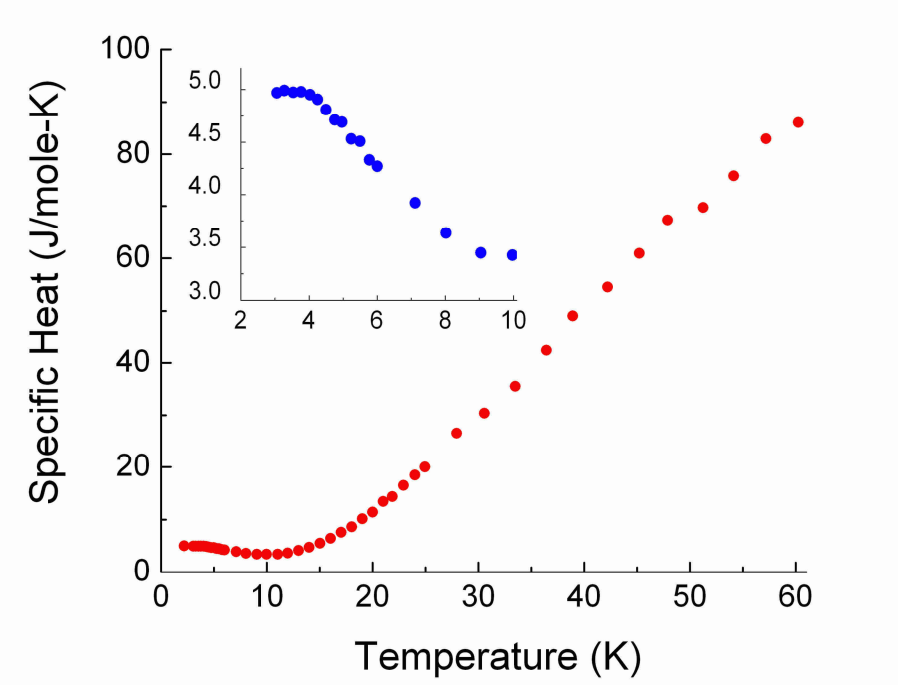

Figure 13: Specific Heat of Yb_4LiGe_4.[8]

Again, the specific heat has the upturn below 10 K (highlighted by the inset), which indicates that there is some magnetism inherent in Yb_4LiGe_4. So although the magnetization measurements did not demonstrate the onset of magnetic ordering at T = 1.8 K, the specific heat data does point to some sort of magnetism at low temperatures. Additionally, specific heat experiments were performed with applied fields up to 3 T. The results are similar in nature to the zero-field data. This could imply that a 3 T field is not sufficiently above a possible $B_{critical}$ for the magnetic behavior of the compound.

Magnetic Susceptibility

To complement the magnetization measurements, magnetic susceptibility measurements were performed on Yb_4LiGe_4. The results are shown in Figure 14 and are plotted again as inverse susceptibility in Figure 16.

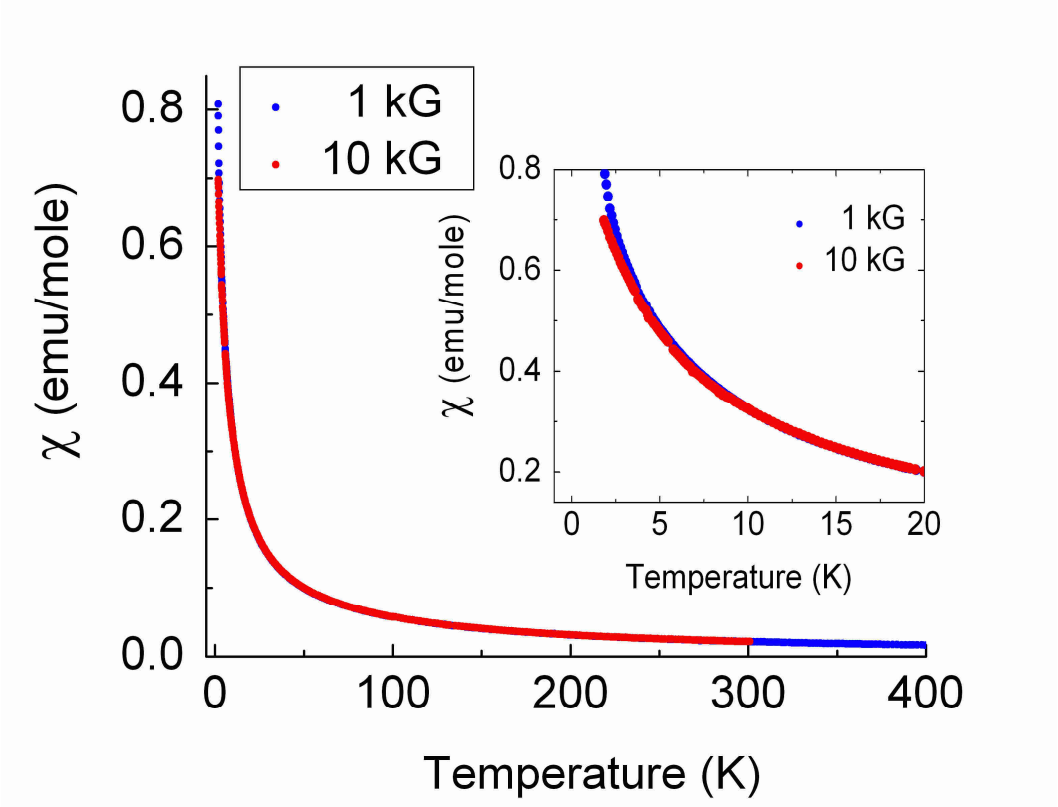

Figure 14: Susceptibility of Yb_4LiGe_4.[8]

Figure 14 looks similar to Figure 5 of the susceptibility for the parent compound for high temperatures, but it lacks the kink in the curve at low temperatures. The high temperature parts of the curves look similar because both compounds behave according to the Curie-Weiss Law. Also, it makes sense that Figure 14 is missing the kink because these measurements were done for T > 1.8 K; and as we saw in the magnetization data, there is no magnetic ordering at those temperatures, hence no maximum in the curve.

Another feature to notice is that when comparing the data for the susceptibility with an applied field of 1 kG (.1 T) with the susceptibility for an applied field of 10 kG (1 T), the 1 kilogauss susceptibilities are slightly higher at low temperatures. But one might think that the susceptibility should be higher with the greater applied field, since it would persuade more magnetic moments to line up. To propose a solution to this quandary, it is necessary to look at the derivation of susceptibility without using an approximation for the magnetization.

From above, $M = N\mu \tanh(\frac{\mu B}{k_B T})$ and $\chi = \frac{\mu_0 M}{B}$, so

$\chi = \frac{N\mu_0 \mu \tanh(\frac{\mu B}{k_B T})}{B}$. Figure 15 shows a plot of this form of susceptibility:

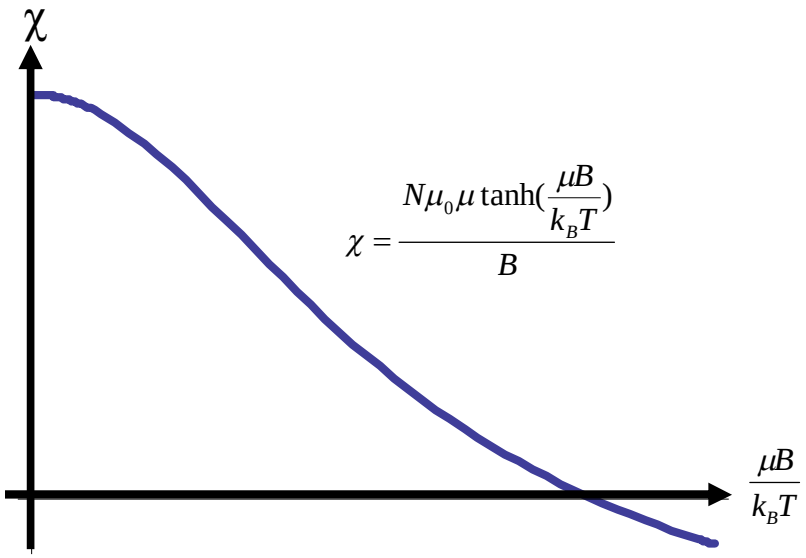

Figure 15: Theoretical Plot of Susceptibility.

So, at low temperatures, the susceptibility will be greater when the applied magnetic field is smaller, which coincides with Figure 14. Now, to draw out more conclusions, looking at inverse susceptibility is useful.

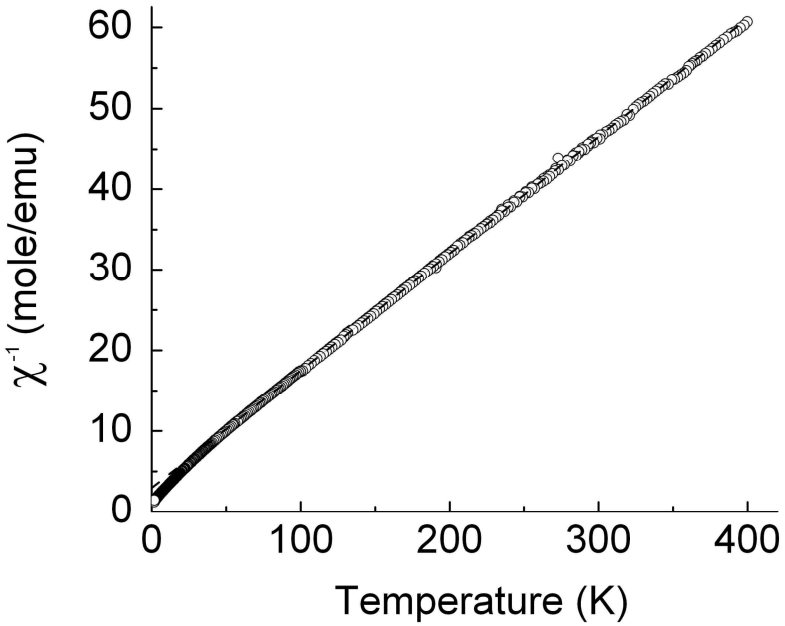

Figure 16: Inverse Susceptibility of Yb_4LiGe_4.[8]

As mentioned, the susceptibility exhibits Curie-Weiss behavior above 60 K. This behavior is more easily seen from the linearity of χ^{-1} in Figure 16, since $\chi^{-1} \propto (T - T^*)$. From curve fits, this data yields an intercept for the temperature axis at T* = -3 +/- 0.1 K.[8] From the earlier discussion, a negative value of T* implies possible antiferromagnetic ordering, similar to the parent compound.

There is a visible deviation from the high-temperature straight line as temperature go below 60 K. Then why is the curve fitted to the high-temperature data? Mathematically, it comes back to the approximation used in the derivation of susceptibility. The Curie Law was derived for $\mu B / k_B T << 1$, which means that the temperature must be relatively high. Physically, the answer is that at low temperatures, the bulk properties of the susceptibility are less dominant.[12]

From the slope of the high-temperature inverse susceptibility data, the effective magnetic moment can be calculated to be 1.86 +/- 0.03 μ_B / Yb.[8] This value is lower than the effective moment of the parent compound discussed above, which may imply that the lithium ions in the sample of Yb_4LiGe_4 have substituted for more of the magnetic Yb^{3+} ions than the non-magnetic Yb^{2+} ions. Further evidence for this hypothesis comes from calculating the ratio of the two ytterbium ions.

To perform the calculation of the fraction of each ion, one uses the equation

$$\mu_{eff} = \left[n_{2+} (\mu_{2+})^2 + (1 - n_{2+})(\mu_{3+})^2 \right]^{1/2}$$

where μ_{eff} is the effective magnetic moment calculated from the slope of the inverse susceptibility, n_{2+} is the fraction of Yb^{2+} ions present, $n_{3+} = (1-n_{2+})$ is the fraction of Yb^{3+} ions present, $\mu_{2+} = 0\ \mu_B$ is the theoretical free magnetic moment for Yb^{2+}, and $\mu_{3+} = 4.54\ \mu_B$ is the theoretical free magnetic moment for Yb^{3+}.[8] Rearranging, one finds:

$$n_{2+} = -\left(\mu_{eff}{}^2 - \mu_{3+}{}^2\right)/\left(\mu_{3+}{}^2\right)$$

which gives a value of n_{2+} = 0.847 +/- 0.005, and thus n_{3+} = .15.[8] Then, the Yb^{3+} ions constitute 15% of all of the ytterbium ions in Yb_4LiGe_4, which is much less than the percentage in Yb_5Ge_4. This is expected since it seems as though magnetic ordering of the parent compound has been reduced or suppressed by the substitution of lithium.

It is also possible that the decrease in the number of Yb^{3+} ions was caused by something other than the preference of the lithium ion's substitution. One other prospect is geometric spin frustration. This type of frustration occurs when the geometric structure of the lattice prevents spins from aligning how they would like to align. A simplified cartoon of this effect is shown in Figure 17.

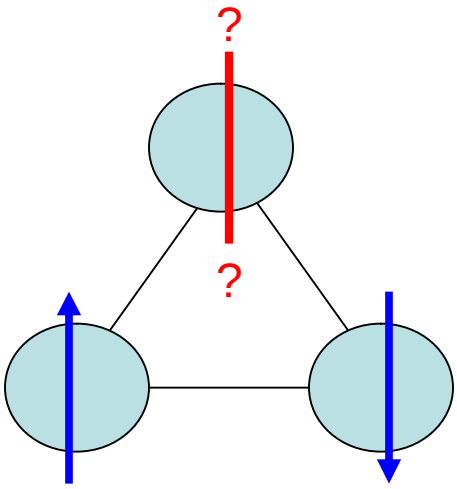

Figure 17: Geometric Frustration for an Antiferromagnet.

Imagine an antiferromagnetic compound with a crystal lattice in the shape of Figure 17. Then, if the bottom two spins want to line up in an anti-parallel fashion, what is the top spin supposed to do? It wants to point down to be anti-parallel to the bottom left spin, but it wants to point up to be anti-parallel to the bottom-right spin. The spins are frustrated because it is not simple for the spins to align like an antiferromagnet.

It turns out that the ytterbium ions form a Shastry-Sutherland lattice, which can lead to geometric spin frustration.[8] Then, this frustration may be the cause of the reduced magnetic moment of Yb_4LiGe_4.

Resistivity

The susceptibility data shows evidence for a possible antiferromagnetic transition, albeit with a reduced magnetic strength. Then at what temperature might this transition be? A clue may come from resistivity data.

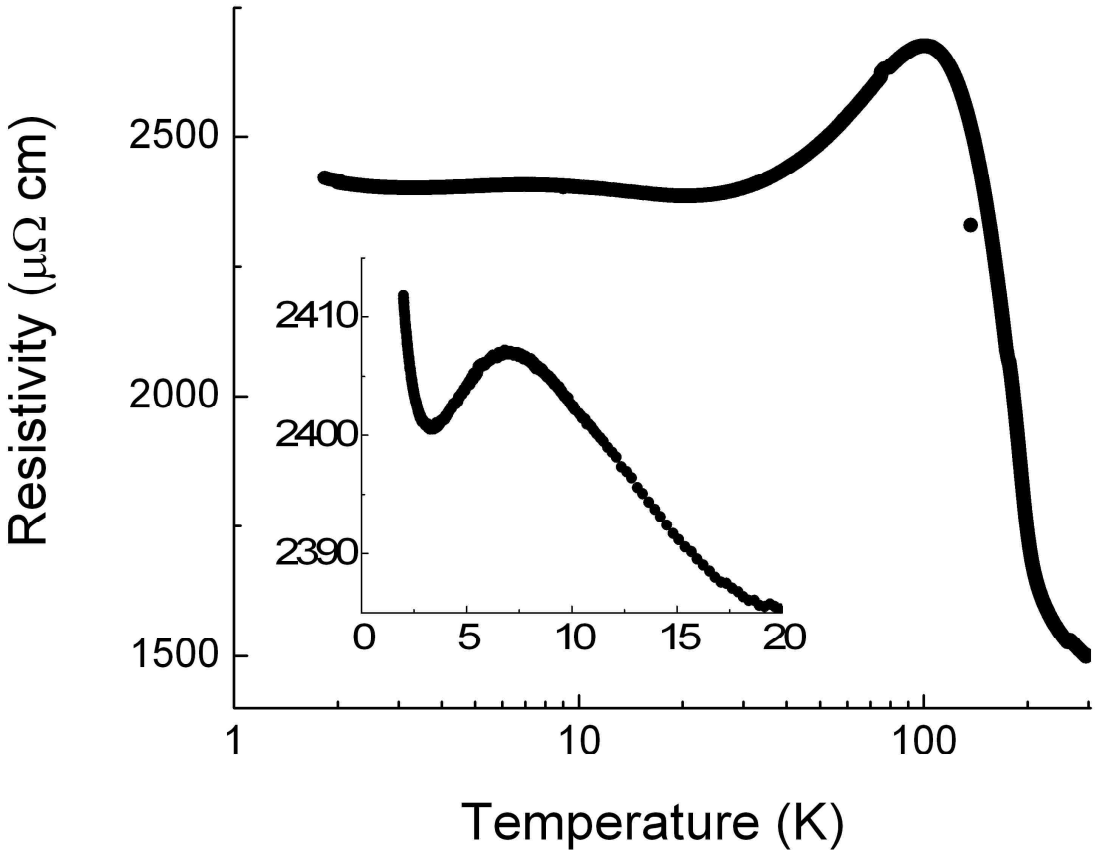

Figure 18: Resistivity of Yb_4LiGe_4.[8]

Figure 18 shows two distinct bumps in the resistivity curve. Oftentimes, these kinds of bumps imply some sort of crossover behavior. They could indicate magnetic ordering,

phase changes, or some sort of change in energy scales. Thus, if Yb_4LiGe_4 orders magnetically, there should be a bump in the resistance curve at the ordering temperature.

The bumps in Figure 18 correspond to temperatures of about 7 K and 100 K. The magnetization data shows that the compound is not magnetically ordered at temperatures above 1.8 K, though. Hence, these bumps must not indicate a magnetic transition. There is one more bump in the curve below 1.8 K though.

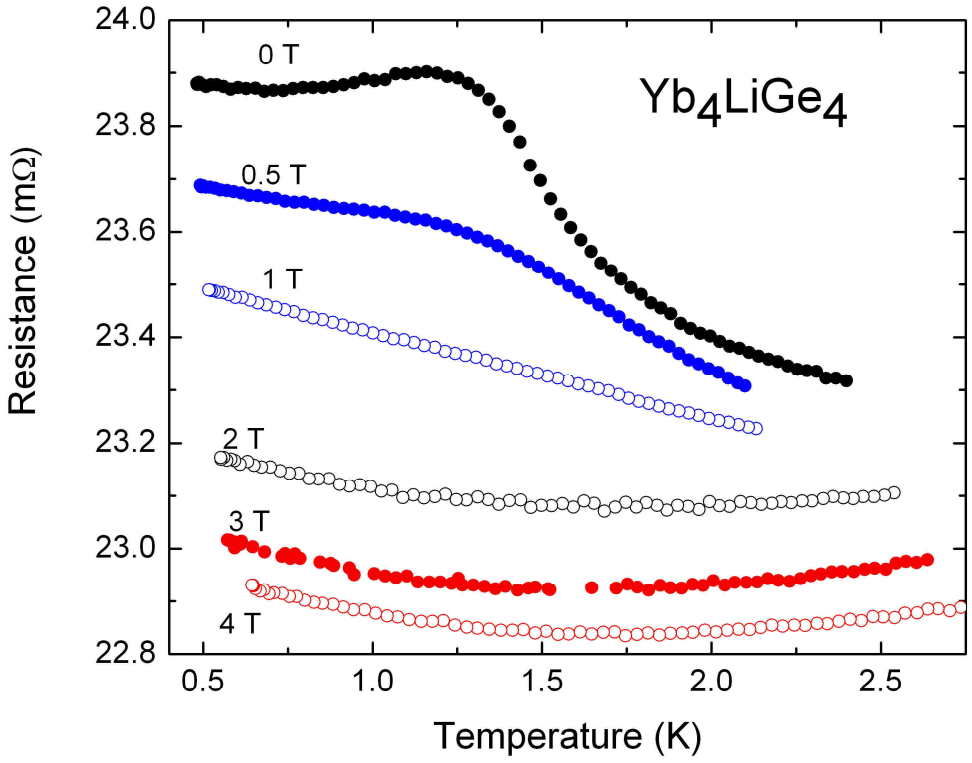

Figure 19: Effect of Magnetic Field on Resistance of Yb_4LiGe_4.[13]

Looking at the 0 T curve of Figure 19, one can see that another bump exists at a temperature between 1 and 1.5 K. Since this temperature is below 1.8 K, it is a candidate for the magnetic ordering temperature. Thus, further investigation of the magnetism at this temperature range is warranted.

Figure 19 also shows the resistance's dependence on the applied magnetic field. When 0.5 T is applied, the bump starts to become suppressed. After 1 T is applied, the resistance curve becomes almost linear for this range of temperatures. It seems as though 1 T is enough to suppress the peak in the resistance for Yb_4LiGe_4, which is just about the same value as the $B_{critical}$ = 1.3 T where the applied magnetic field dominates over the magnetic ordering of the parent compound.

Recent Results

μSR

To probe Yb_4LiGe_4 further for signs of magnetism, Muon Spin Relaxation, or μSR, was utilized. μSR is a great tool to use because it uses particles known as muons to probe local magnetic fields within samples. To better understand how μSR works, then, it is a good idea to start by better understanding muons.

Muon Production

In order to have a steady source of muons, it is essential to have a particle accelerator. The experiments performed on Yb_4LiGe_4 were all done in the ISIS Rutherford Appleton Laboratory in Didcot, England, using their synchrotron accelerator, muon beam, and measurement devices. Synchrotrons use electric fields to accelerate charged particles ($\vec{F} = m\vec{a} = q\vec{E}$) and magnetic fields to bend the beam path ($\vec{F} = q\vec{v} \times \vec{B}$).

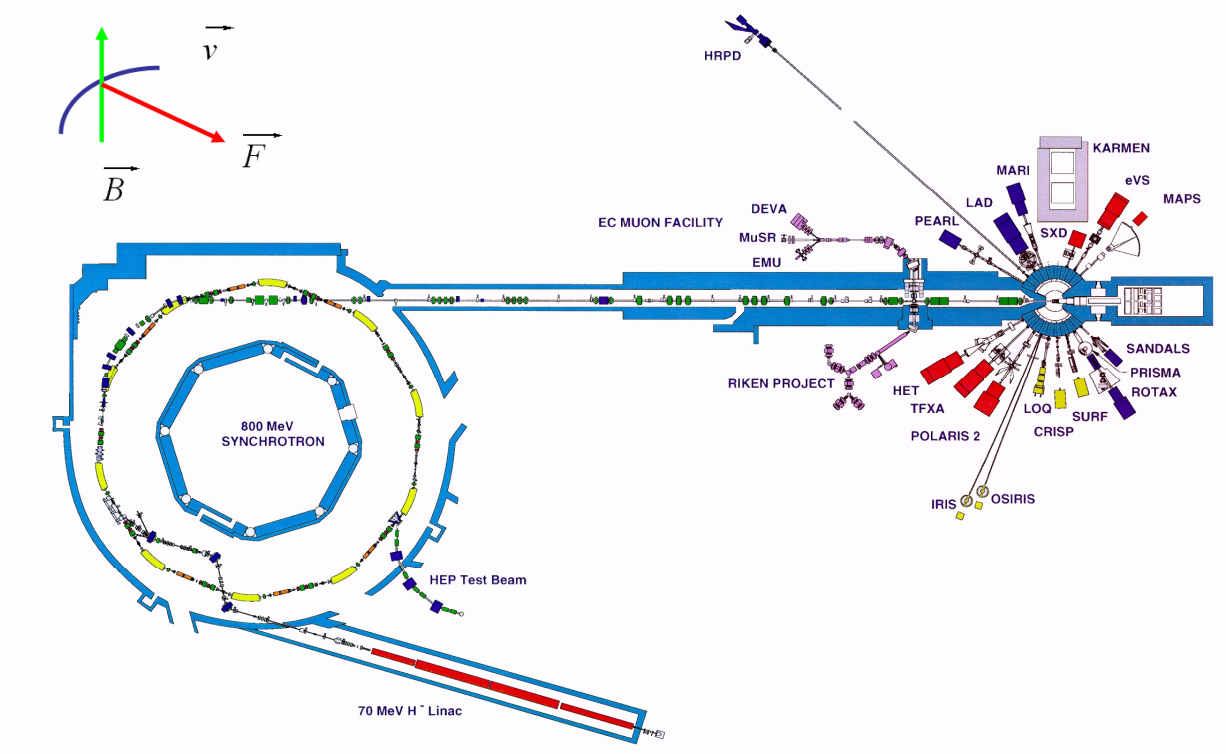

Figure 20: Synchrotron at ISIS.[14]

The charged particles that the ISIS synchrotron accelerates are protons that originate from hydrogen atoms that are stripped of their electrons by aluminium oxide foil.[14] Then these protons hit a graphite target, colliding with nuclei to form pions. This target is chosen because it has a low number of nucleons, which reduces beam scatter, and because of its high melting point, which is necessary because of the high amount of energy present due to the collisions.[15] The pions then decay with an average lifetime of 26 nanoseconds into a muon and a neutrino: $\pi^+ \rightarrow \mu^+ + \nu_\mu$.[15]

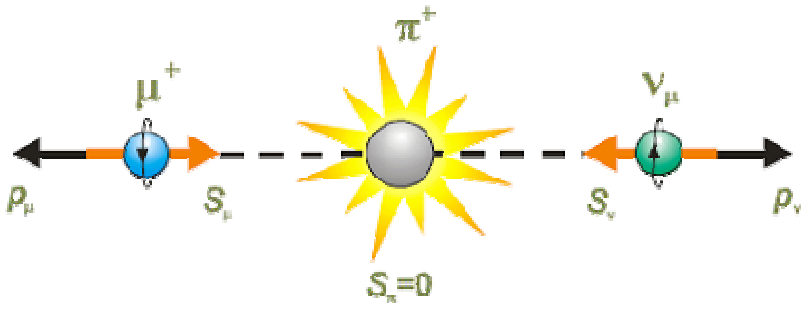

Figure 21: Pion Decay.[16]

Due to the non-conservation of parity in weak interactions (weak forces are the reason for this decay), the neutrinos formed are "left-handed particles."[17] To say that they are left-handed means that their spin always points in the opposite direction of their linear momentum. Then, upon conservation of linear and angular momentum, the newly created muon also has its spin (S = ½) point oppositely from its linear momentum. Thus, the muon beam that results from the pion decays become 100% polarized. If all the muons in the muon beam are going forward, then all of their spins are pointing backward.

Muons in Materials

The muon beam subsequently gets directed to the sample, which is Yb_4LiGe_4 in this case. When a muon enters the sample, it stops in an interstitial site because of its positive charge.[18] Here, the muon feels the effect of the local magnetic field because of its own magnetic moment which comes from its spin and charge (one positive elementary charge). In a static field, the muon will begin to precess.

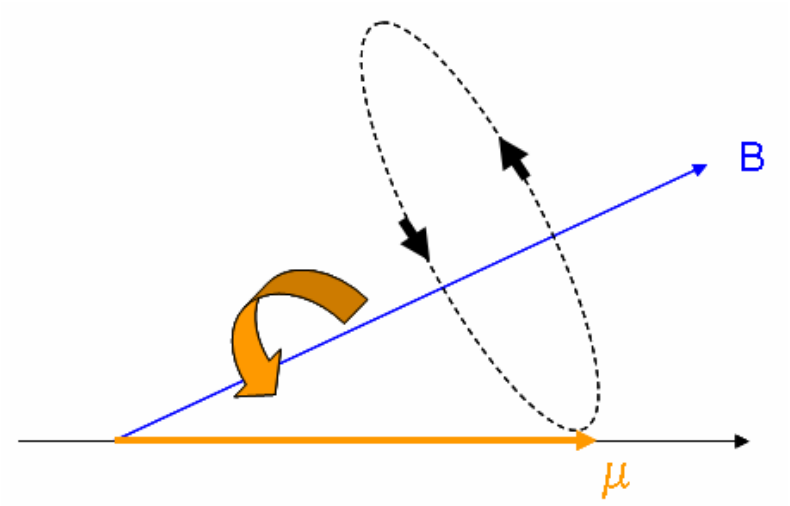

Figure 22: Precession due to Magnetic Torque.

The precession is called Larmor precession. Then, the angular frequency $\omega = 2\pi\nu_\mu = \gamma_\mu B$, where ν_μ is the precession frequency and γ_μ = 851.6 Mrad s^{-1} T^{-1} is the muon

gyromagnetic ratio.[18] The Larmor precession will change the direction of the magnetic moment of the muon in a sinusoidal fashion. Then, after an average lifetime of 2.2 μs, the muon will decay into a positron, a neutrino, and an antineutrino: $\mu^+ \rightarrow e^+ + \nu_e + \overline{\nu_\mu}$.[15]

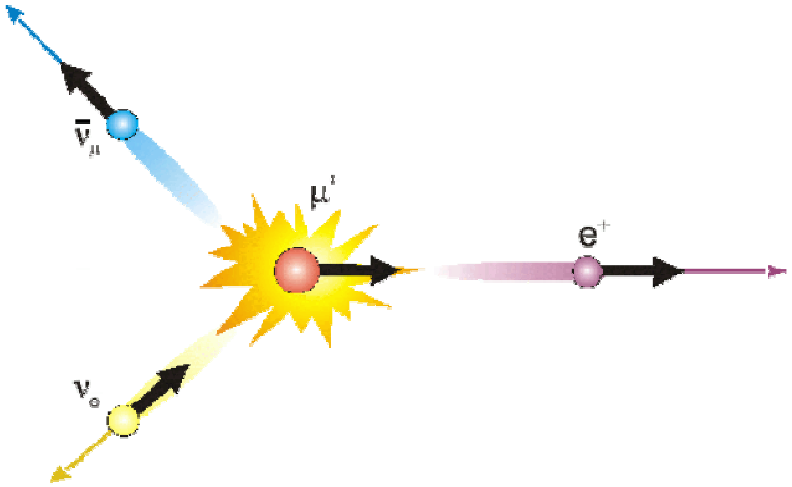

Figure 23: Muon Decay.[16]

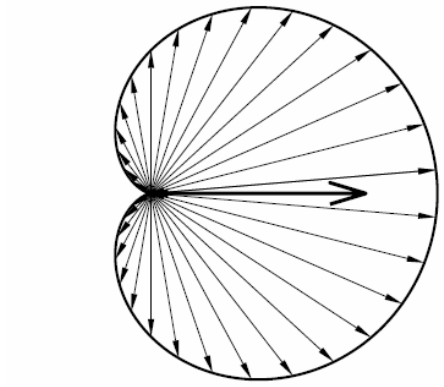

Figure 24: Expected Angular Direction for Positron, Where Dark Arrow is the Muon Spin Direction.[19]

Once again, parity violation of the weak interactions involved in this decay lead to the positron being emitted preferentially in the direction of the muon spin.[19] Then, one of the

sixty-four detectors surrounding the sample detects the emitted positron. The detectors are grouped together as either forward or backward detectors, as seen in the following photo.

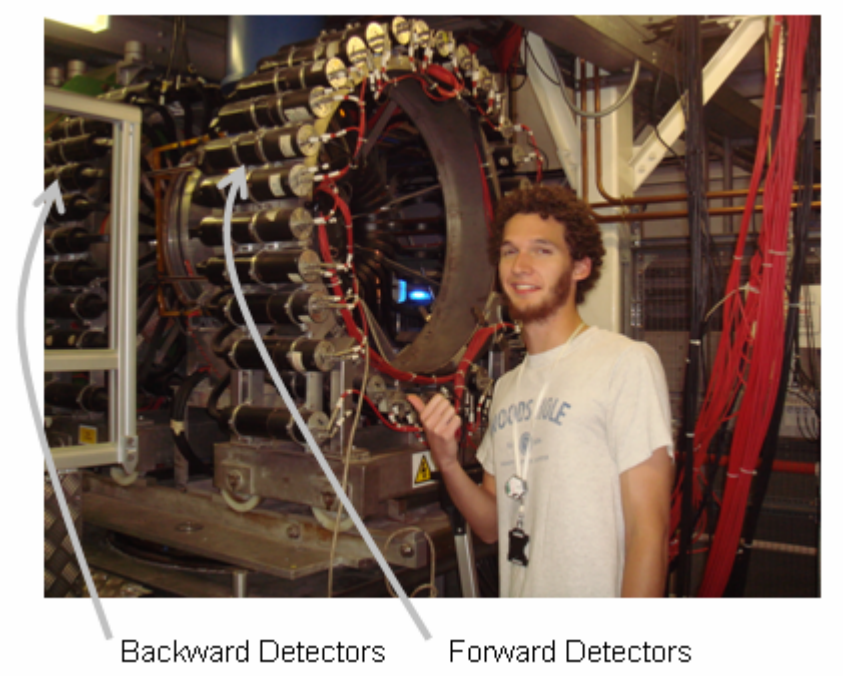

Figure 25: Niclas Svensson with Positron Detectors

Muon Experiments

In an actual experiment, millions of muons are counted. There are two different ways to send so many muons into the sample: continuous muon beam and pulsed muon beam. In the continuous muon beam mode, a single muon enters the sample, starts a clock, decays into a positron emission, and then the positron is detected and the clock stops. If another muon enters the experiment while the first is still around, though, then neither positron detection can be counted. In the pulsed muon beam mode, a clock starts when millions of muons are sent into the sample simultaneously in an intense pulse. Then, each event, or detection, is timed with respect to the collective start time. Thus, muons with a longer-than-average lifetime can still be detected, unlike in the continuous muon beam case. The experiments at ISIS used pulsed muon beams.[19]

So, once the millions of positrons from the millions of muons that are sent into the sample get detected, the experimenter can observe the asymmetry. The asymmetry is basically the normalized difference between the number of positrons detected by the backward and forward detectors. It takes the form: $A(t) = \frac{N_B(t) - N_F(t)}{N_B(t) + N_F(t)}$, where A(t) is the asymmetry, $N_B(t)$ is the number of positrons detected by the backward detectors, and $N_F(t)$ is the number of positrons detected by the forward detectors.

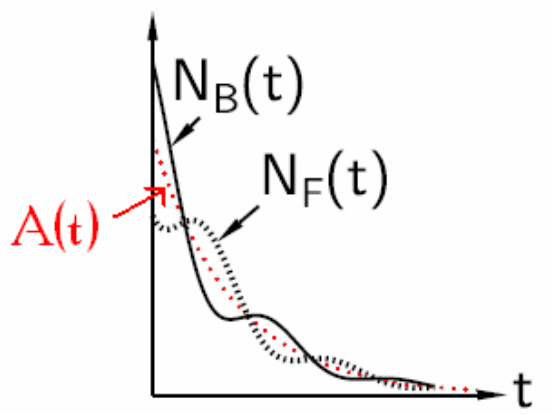

Figure 26: Asymmetry Curve.[19]

Once the data for the asymmetry has been collected, the data can be fit to a curve. Some of the possible forms of these curves are the following:

Table 1: Depolarization Functions[16]

Menu of Depolarization Functions		
Gaussian.....	$\cos(\omega_\mu t + \phi)\exp\left(-\Delta^2 t^2/2\right)$	TF
Fluctuating Gaussian.....	$\cos(\omega_\mu t + \phi)\exp\left(-\Delta^2 t/\nu\right)$	TF
Kubo-Toyabe.....	$\frac{1}{3}\left[1 + 2(1-\Delta^2 t^2)\exp\left(-\Delta^2 t^2/2\right)\right]$	ZF
Kubo-Lorentz.....	$\frac{1}{3}\left[1 + 2(1-\Delta t)\exp(-\Delta t)\right]$	ZF
Fluctuating moments.....	$\exp(-\lambda t)$	ZF, LF
Fluctuating dilute moments	$\exp\left(-(\lambda t)^{1/2}\right)$	ZF, LF

The fit function can also be a sum of more than one of these depolarization functions. The term "depolarization" arises because it is a measure of how long it takes for the complete polarization of the spins in the muon beam to deteriorate into separate directions. In other words, the initial strict alignment of the muon spins relaxes into a collection of different orientations. This "relaxation" is the "R" in μSR.

In Table 1, TF stands for Transverse Field, LF is Longitudinal Field, and ZF is Zero Field. These fields refer to the magnetic field applied to the sample. In transverse field mode, the magnetic field is in a direction perpendicular to the muon beam's direction. It is often necessary to do a calibration measurement of a few million events in a transverse field of 20 gauss before running in longitudinal field mode.[20] Longitudinal field mode uses an applied magnetic field in the direction of the muon beam polarization.

The third mode, zero field, does not just mean that there is no applied field. In fact, zero field takes into account ambient magnetic fields, like the earth's, and applies a small field to cancel them. But is the earth's magnetic field really that large? Well, it is only on the order of 10^{-5} Tesla.[21] However, muons are sensitive to fields as low as 10^{-5} Tesla because of their large magnetic moments, which is why it is necessary to compensate for other fields in order to get a true zero field.[19]

μSR Measurements

Examples of the asymmetry data for Yb_4LiGe_4 are shown in Figure 27. The blue line represents the depolarization curve that was fitted to the data. The function that was used for this compound is of the form

$$A(t) = A_1 e^{-(\lambda_F t)^{1/2}} + A_2 e^{-(\lambda_S t)}$$

where $A_1 \approx A_2$. Thus, the function is a sum of fluctuating moments' and fluctuating dilute moments' theory functions.

For this fitting function, there are two λ's, which are the relaxation rates. Both the fast rate, λ_F, and the slow rate, λ_S, were varied as parameters when fitting the curves. But why are there two different rates? Apparently, there are two components to the muon behavior that relax differently in time.

What does this mean physically? There are a couple possibilities. Although oftentimes muons tend to congregate in one certain spot in a lattice structure, the two lambdas may indicate that there are two preferred interstitial stopping points for the muons in Yb_4LiGe_4. Alternatively, the muons may all go to the same crystallographic location, but the lithium ion might have substituted into different ytterbium sites for different molecules. Or, along the same lines, the Yb^{3+} ions

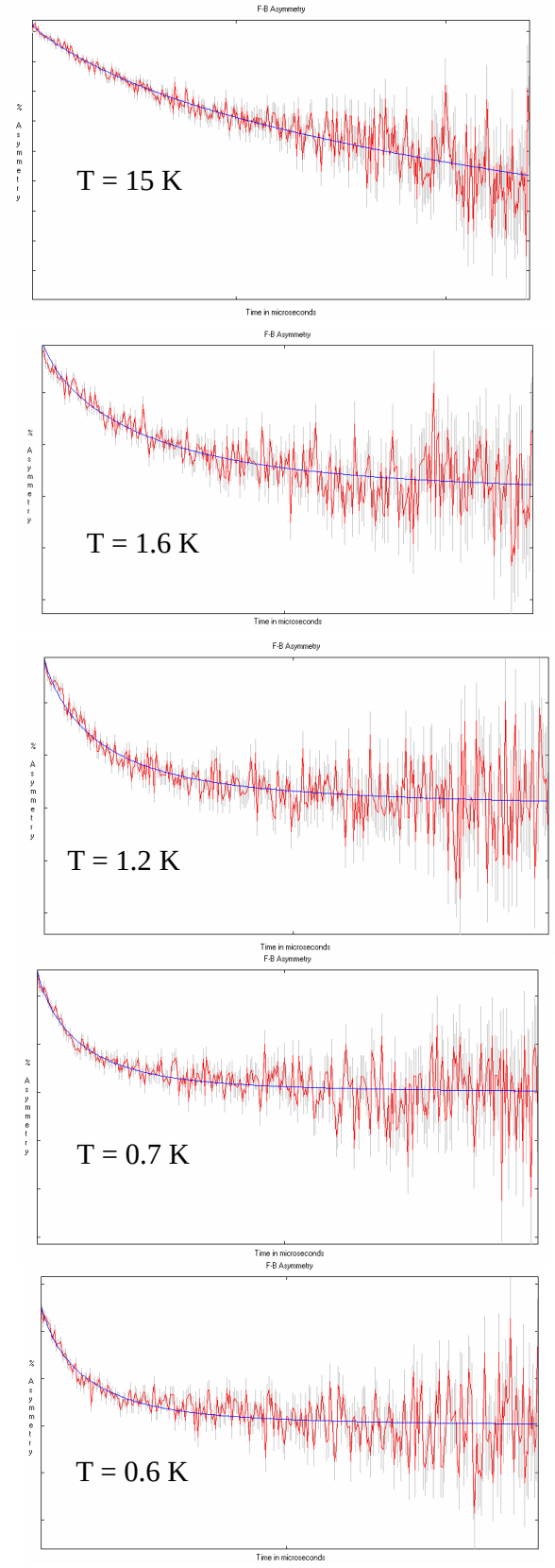

Figure 27: Depolarization Curves at Different Temperatures.

may reside in different ytterbium sites for different molecules. Then the same point in the lattice could have different local behaviors. Any of these situations, or even a combination of more than one of them, has the potential to cause the two different relaxation rates.

Whatever the case may be, the depolarization function is fit to the asymmetry for a certain temperature, and both relaxation rates are recorded. Then, this process is repeated at different temperatures. After the experiment has run at a range of temperatures, the relaxation rates are plotted. Figure 28 shows the results of muon spectroscopy on Yb_4LiGe_4 for temperatures between .06 and 2 K.

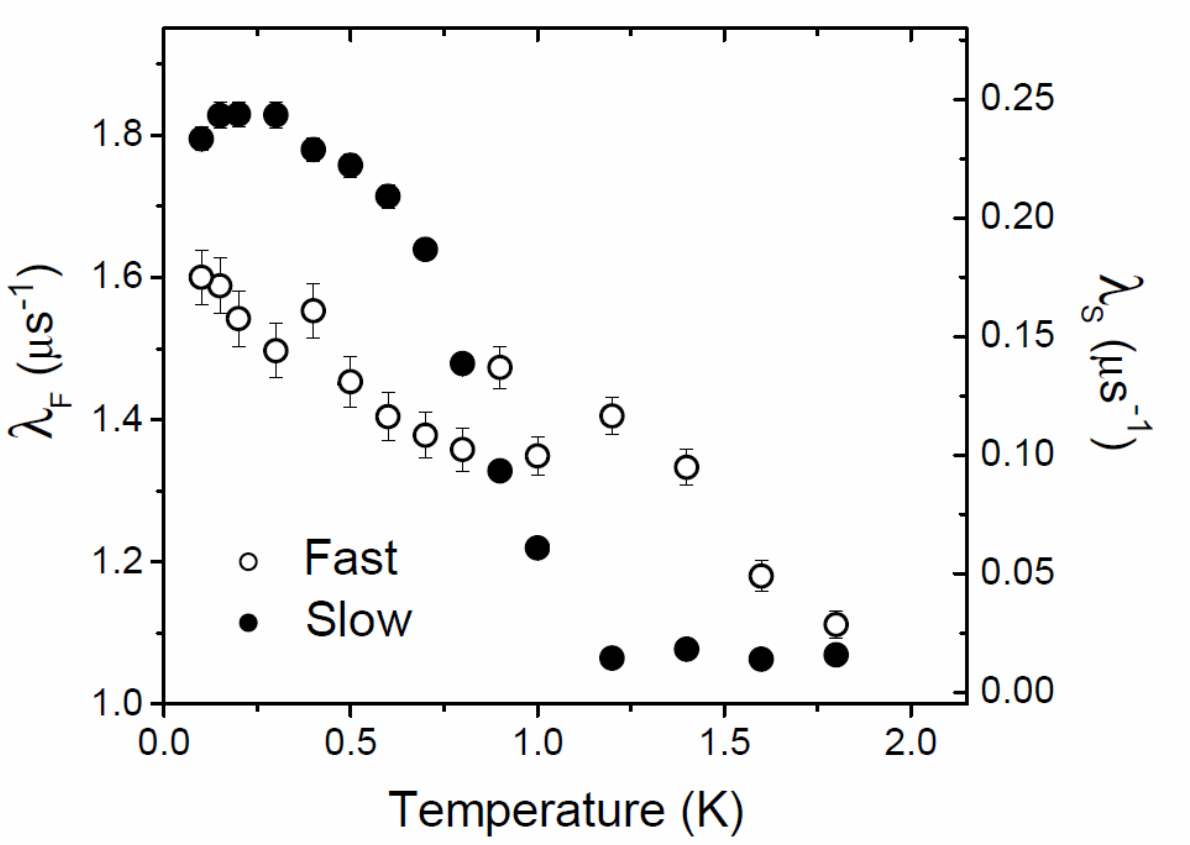

Figure 28: Results of μSR Experiments.

Figure 28 plots both relaxation rates versus temperature. The λ_F points (filled in circles) do not reveal any qualitative data. However, one can see that the λ_S does. At

temperatures between 1.2 and 1.8 K, λ_S stays nearly constant with a value of about 0.02 μs^{-1}. Then, below 1.2 K, the relaxation rates increase dramatically by an order of magnitude. This sudden change indicates an abrupt change in the magnetism of the sample.

Qualitatively, one can see the change in the relaxation rates in Figure 27. Below 1.2 K, the initial drop in the fitted curve is a lot quicker and steeper than above 1.2 K. Sometimes a change like this occurs because of magnetic ordering, but it is not a sufficient condition in order to conclude ordering in Yb_4LiGe_4.[12] Recall, though, that the resistivity data also showed a possible transition near 1.2 K.

Because of the susceptibility data, antiferromagnetism would be an obvious choice for the type of magnetic ordering that may or may not be occurring at 1.2 K. However, other runs of μSR experiments pointed elsewhere. After acquiring some data by running an experiment with an applied magnetic field, then running without the field, and then running the initial experiment with the same initial applied field, the data did not match up. It turns out that hysteresis had taken place. Now, remember that hysteresis is a signature of ferromagnetism. Then this result is very interesting because it conflicts somewhat with the conclusions made from the susceptibility measurements.

It is possible that competition between ferromagnetism and antiferromagnetism exists in Yb_4LiGe_4. This competition could explain the presence of both the ferromagnetic and antiferromagnetic effects. It is also notable to add that geometrically frustrated magnets oftentimes display this type of competition, which makes this explanation even more plausible.[8]

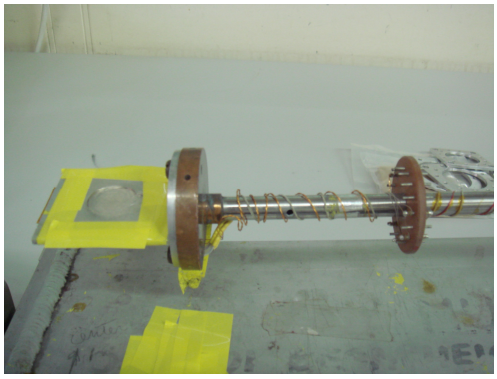

Figure 29: Sample Holder for μSR Experiments.
(the silver plate backing is used because silver does not leave a substantial magnetic signature)

Resistance Measurements with Sample under Pressure

The susceptibility, resistivity, and μSR measurements indicate some sort of magnetic ordering for Yb_4LiGe_4 at a temperature of approximately 1.2 K. This possible Néel Temperature is half a degree below that of the parent compound. Thus, the substitution of a lithium ion has a definite effect on the magnetism of Yb_5Ge_4. The next test that was performed to probe this magnetism was resistivity measurements with the sample under pressure. The questions being asked are, will pressure act to reverse the effects of the substitution, will it enhance the effects of the substitution, or will pressure have no effect on the compound's magnetic properties?

Why should pressure have any effect at all? Well, applying pressure changes the crystalline structure, and R_5T_4 compounds are very sensitive to these changes. The pressure could shift the positions of parts of the lattice, or push ions and molecules closer, making the magnetic moments have more effect on each other. Or pressure might compress the compound with little effect on the magnetic properties. The result is unknown, which is why it is interesting to investigate.

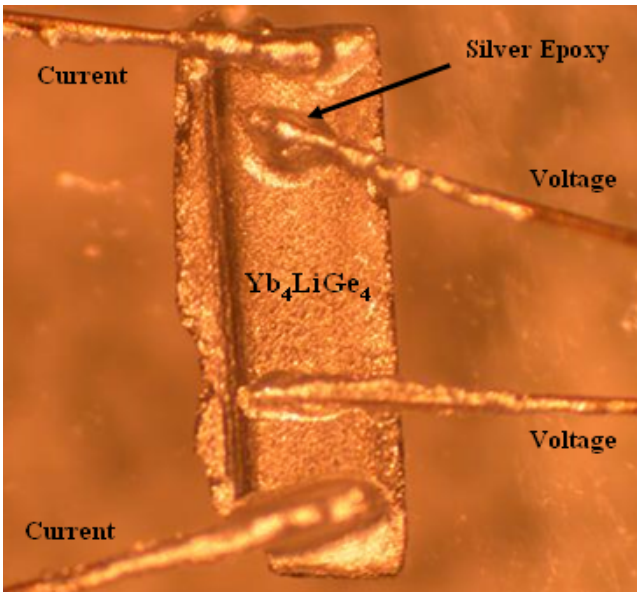

Figure 30: Yb_4LiGe_4 Sample with Brass Wires Attached by Silver Epoxy

The Pressure Cell

To apply pressure to the sample, a copper-beryllium pressure cell was used. The sample resides in the cell and is immersed in a pressure transmitting medium. Then, decreasing the volume of the medium increases the pressure on the sample. The applied pressure is hydrostatic, meaning the static fluid applies pressure to all sides of the sample. Electrical connections within the cell allow for resistance measurements to be performed.

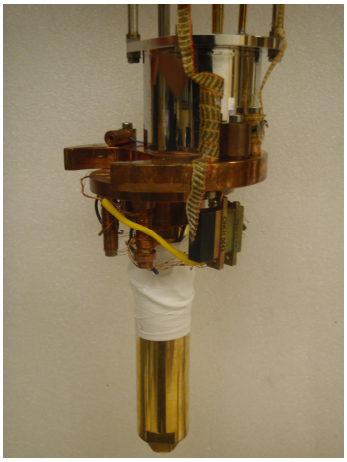

Figure 31: The Pressure Cell Connected to the Dilution Refrigerator.

Dilution Refrigerator

Before going into the results of the low-temperature resistance measurements of the sample under pressure, it is important to understand how such low temperatures were reached. At Boston College, a Kelvinox MX50 Dilution Refrigerator made by Oxford Instruments was used because of its ability to reach temperatures in the millikelvin range. How a dilution fridge works is somewhat complicated with a simple idea behind it.

Principles Behind a Dilution Refrigerator

Figure 32: The Dilution Refrigerator.

The dilution refrigerator (and sample) starts off at room temperature, and then is cooled to the temperature of liquid nitrogen, and subsequently, to the temperature of liquid helium, T = 4.2 K. Then, pumping on the 1 K pot (see diagram of fridge in Appendix F) cools it further so that it condenses a mixture of about 6% ^{3}He and 94% ^{4}He into the dilution refrigerator.[22]

The mixture moves into the mixing chamber where a phase boundary is set up once the temperature goes below 0.86 K; this temperature is reached by pumping on the still.[22] The

boundary exists between a ^{3}He-rich side and a ^{3}He-poor side. The ^{3}He-rich side is the concentrated phase and can be regarded as "liquid ^{3}He," while the ^{3}He-poor side is the dilute phase and can be regarded as "^{3}He gas." Obviously, the dilute phase is mostly ^{4}He. When the dilute phase is pumped on in the still, however, mostly ^{3}He is removed because its vapor pressure is about 1000 times higher than that of ^{4}He.[22] Then, the equilibrium is disturbed. In order to regain equilibrium, ^{3}He from the ^{3}He-rich phase must cross over to the dilute phase. Thus, the liquid phase must be transformed into the gas phase, which takes energy. This energy is taken by absorbing heat from the fridge, effectively lowering the fridge's temperature.

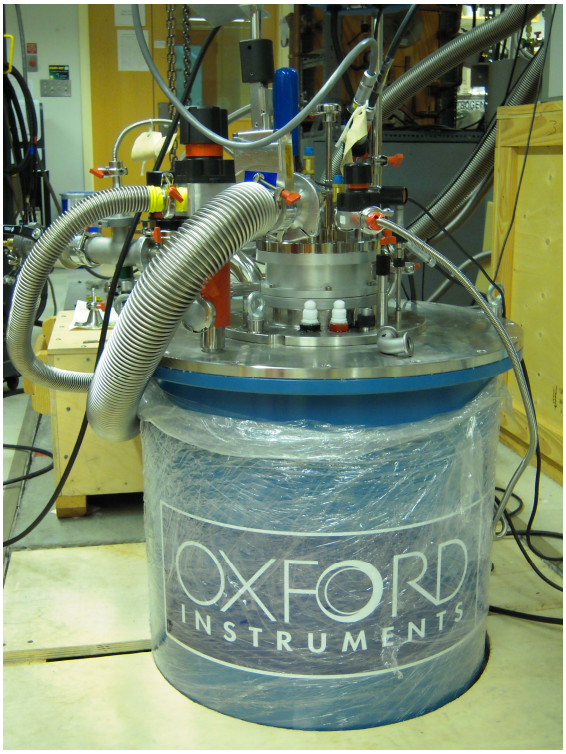

Figure 33: Outside of Dilution Refrigerator.

It is easy to forget the fine details of how a dilution refrigerator works. Basically, though, a dilution fridge cools down for the same reasons that a gust of wind chills someone

who has just gotten out of the pool. The evaporation of the liquid occurs by absorbing energy from the heat it draws away from its surroundings.

Pressure Dependence of Resistance

The first experiment done with Yb_4LiGe_4 in the dilution refrigerator was designed to have zero pressure applied to the sample at low temperatures. That way, the resistance curve could be compared to the curve in Figure 19 obtained earlier from cooling the compound in a different refrigerator without the pressure cell.

In order to achieve zero pressure at low temperatures, the pressure cell was pressurized to a value of about 4 kbar because previous experiments had shown that a pressure of 4 kbar will lead to a zero pressure measurement at low temperatures. Why is any pressure necessary if zero pressure is desired? The pressure cell is pressurized to help prevent air bubbles from forming in the pressure transmitting medium.

The two curves match up, which implies that the pressure cell does not distort the results. The resistance curve with the pressure cell is shown in Figure 34. Notice the bump in the resistance at about 1.2 K. The temperature of the bump is the same as the temperature at which the μSR data showed an abrupt change in the magnetic ordering.

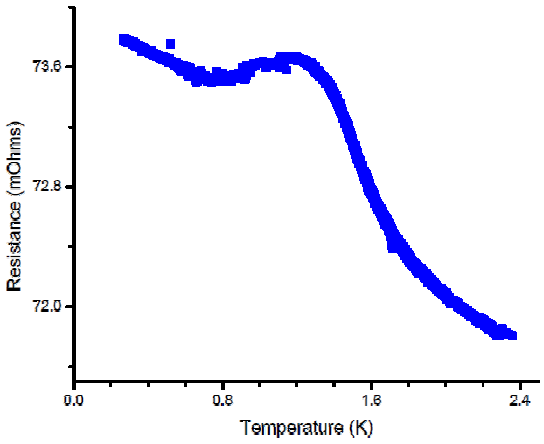

Figure 34: Zero Pressure Resistance Data.

After confirming that the addition of the pressure cell does not affect the resistance measurements, the sample was measured under three additional pressures. The pressures at room temperature and at liquid helium temperature are compared in Figure 35.

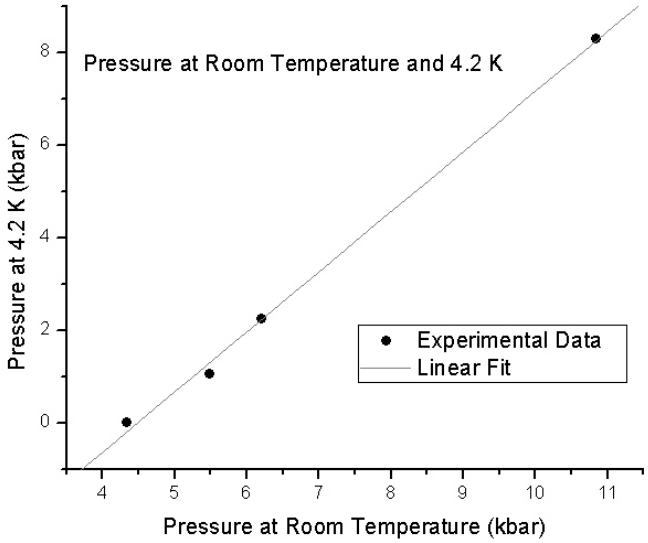

Figure 35: Pressure at Room Temperature vs. Pressure at 4.2 K.

The pressures (in kbar) are approximately related by the equation $P_{4.2K} = 1.30 \cdot P_{RT} - 5.81$. The data for the resistance measurements for all four pressures is plotted below.

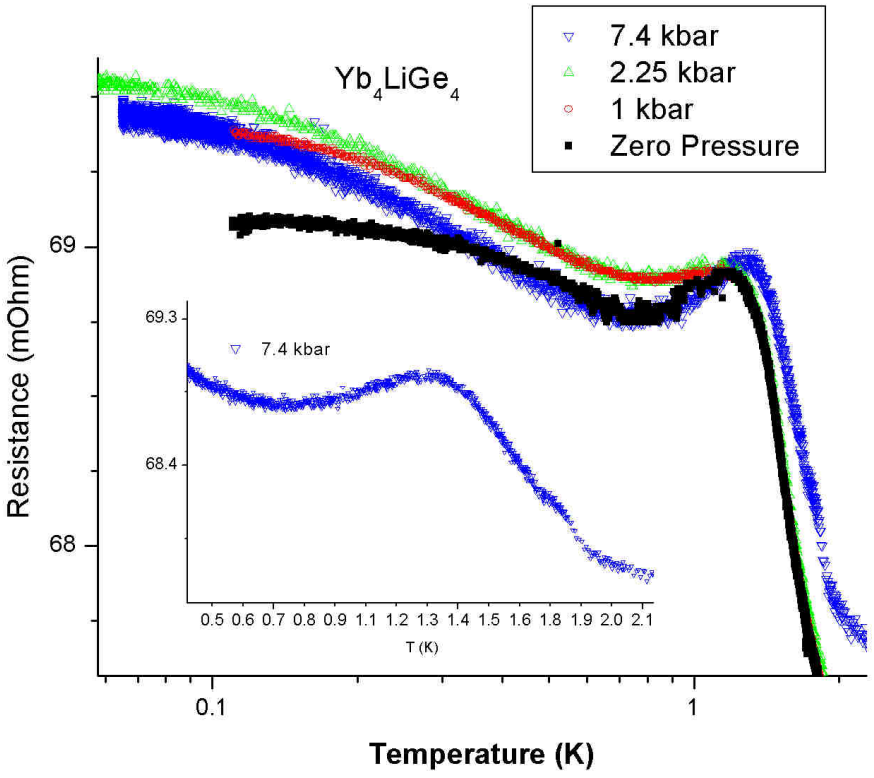

Figure 36: Resistance Data for Four Pressures.
(Note that a constant may have been subtracted in order for the data to lie in the same range in order to show the qualitative nature.)

Obviously, increasing the pressure to 1 and 2.25 kbar did not shift the bump to a different temperature. The only noticeable difference between these curves is that the humps broaden slightly. In other words, the bump is less steep. The mostly ineffectiveness of applying 2.25 kbar of pressure is surprising since R_5T_4 compounds are very sensitive to changes in pressure, and because some compounds containing ytterbium ions, such as $YbCu_{3.5}Al_{1.5}$, are also sensitive.[23] Thus, a shift of the possible Néel Temperature would be expected.

This shift is witnessed in the 7.4 kbar data. Applying 7.4 kbar of pressure to Yb_4LiGe_4 may not change the resistance curve much, but there are definite qualitative and quantitative changes. It is interesting that this data shows a sharper bump with a steeper drop-off in the

resistance after the maximum. This behavior is opposite to the behavior observed when the pressure was increased from zero pressure to 1 or 2.25 kbar. Those curves had broader, less dramatic bumps than the zero pressure one. But it seems as though increasing the pressure even more returns the steepness of the bump.

The quantitative change in the 7.4 kbar data is the shift in the maximum. The maximum changes from 1.2 K to 1.3 K. Thus, if 1.2 K is a Néel Temperature for Yb_4LiGe_4 without any applied pressure, then 1.3 K is the compound's Néel Temperature under 7.4 kbar of pressure. This temperature is higher, and thus slightly closer to the transition temperature for the parent compound.

Higher temperatures mean greater thermal agitations for the spins. So, a higher ordering temperature, if it is an ordering temperature, indicates that the magnetism in the compound under pressure is stronger since it dominates over stronger thermal spin agitations. Substituting lithium decreases the magnetic strength of Yb_5Ge_4. Thus, the application of pressure serves to reduce the effect of substituting lithium.

If the relation between the change in the ordering temperature and the applied pressure is linear, then more than 35 kbar would be required to give Yb_4LiGe_4 the same ordering temperature. However, it is not necessarily wise to assume linear behavior since only the 7.4 kbar data yielded any noticeable shift in the resistance curve's maximum.

Why did the transition temperature rise when pressure was added? It is possible that this effect occurred because of the difference in sizes of the two kinds of ytterbium ions. Pressure compresses the crystals of the compound, which means that the smaller sized ions would fit in more easily. If this is the case, then the Yb^{3+} ions, which have smaller radii,

would be preferentially present in the lattice rather than the Yb^{2+} ones. Since Yb^{3+} is the magnetic ion, the compound under pressure would have a stronger magnetic moment.

The 7.4 kbar data may reveal something more, though. The inset of Figure 36 shows the emergence of a small bump in the resistance around T = 1.75 K. Recall that the ordering temperature for the parent compound is at 1.7 K. This observation raises some questions. Is it possible that the behavior of Yb_4LiGe_4 at 1.2 K is not the same kind of behavior as that of Yb_5Ge_4 at 1.7 K? In other words, is the antiferromagnetic transition of the parent suppressed entirely with some different type of magnetism appearing in the daughter? This may explain why hysteretic behavior was observed. Another question would be, is this new bump indicative of other types of ordering? Is there any difference between the magnetic properties of the sample under the lower pressures and the 7.4 kbar?

Unfortunately, these questions will remain unanswered for now because it is difficult to perform other types of measurements besides resistance on the pressure cell. Furthermore, it is unclear whether or not more investigation of this small bump is warranted since there is only one dataset for the resistance at a temperature range near 1.75 K. Without further data for reinforcement, the true existence of the bump is somewhat debatable; it could just be error. Also, the pressure cell that was used for all of these measurements is not built for higher pressures, so a further increase in pressure would not be easy.

In any case, the high pressure data is clear about one thing. Increasing pressure increases the ordering temperature of Yb_4LiGe_4.

Conclusion

Yb_4LiGe_4 is an interesting compound to study. Its mixed valence nature, with magnetic Yb^{3+} ions and non-magnetic Yb^{2+} ions, leads to some unusual magnetism. Also, the

material's crystal structure helps to make the compound's magnetic properties even more difficult to predict.

Several experiments were performed at temperatures down to 1.8 K. The results of the magnetization measurements showed that the magnetism of the parent compound had been partly suppressed. However, data on the specific heat of Yb_4LiGe_4 showed that the magnetism had not disappeared entirely. This result was strengthened by the susceptibility experiments.

The high-temperature susceptibility followed the Curie-Weiss Law and implied possible antiferromagnetism in the compound. Also, the magnetic moments of the ytterbium ions were extracted from this data and were found to be smaller than those in Yb_5Ge_4. This means that there are less Yb^{3+} ions in Yb_4LiGe_4, which is why the magnetism is not as strong.

Resistivity measurements indicated that there is a possible magnetic transition at 1.2 K, so new experiments were performed at lower temperatures. μSR studies supported the idea that there might be magnetic ordering at 1.2 K because of an abrupt change in the depolarization of muons at that temperature. μSR also gave evidence for possible ferromagnetism too, though, because of hysteretic behavior observed during runs.

Further probing of Yb_4LiGe_4 at low temperatures came in the form of resistance measurements with the material under pressure. The experiments showed that a substantial amount of pressure was required in order to shift the possible transition to a higher temperature. The pressure may create cites in the crystal lattice which are more ideal for the smaller, magnetic ytterbium ions, which may be why the transition temperature is raised.

Additionally, the observation of an emergence of an supplementary bump in the resistance data opened the door to greater speculation about what is actually being measured at 1.2 K and how the magnetic properties of Yb_4LiGe_4 are related to Yb_5Ge_4.

The unusual magnetic properties of this material may be the result of geometric frustration. It is possible that the shape of the crystals is preventing antiferromagnetism, or any other type of magnetism, from becoming dominant. Thus, there may also be frustration between two or more types of magnetism. This frustration might explain why signatures of both antiferromagnetism and ferromagnetism are present in Yb_4LiGe_4. It is also possible that the compound is experiencing some sort of ferrimagnetism. Ferrimagnets are something of a middle ground between ferromagnets and antiferromagnets.

Further experiments are needed to be able to describe the magnetism of Yb_4LiGe_4 more thoroughly. Currently, new specific heat and susceptibility measurements are being performed at temperatures lower than in previous experiments. Additionally, resistance measurements with greater applied magnetic fields can be performed, as well as resistance measurements with magnetic fields and applied pressure.

This thesis project was a tremendous learning experience for me. The hands-on, practical application of physical concepts and experimental methods supplemented my class work greatly. The work involved gave me a taste of lab work; and despite the difficulties that were encountered throughout my time in lab, I still developed a thirst for it. I learned a lot, but there is a lot more for me to learn.

Appendices

Appendix A: Synthesis

In order to produce samples to work with, the sample preparer started with ingots of 99.99 percent pure ytterbium, rods of 99.4% lithium, and pieces of germanium that were 99.9999% pure. Then, the three elements were placed together into a tantalum tube in a stoichiometric ratio of 4:1:4, which was then sealed and heated to 1073 K with a high frequency furnace. Next, the compound was put into a planetary ball mill. Ball mills are cylinders with a grinding medium inside that rotate, making the grinding medium, which could be something like stainless steel balls, continuously fall onto the material loaded into the ball mill and pulverize it into powder. The compound was ball milled for half an hour at 600-800 rpm. In order to prevent impurities with the ytterbium, and because lithium is moisture sensitive, an argon glove box was used throughout these processes.

Subsequently, the powder was poured into the tantalum foil-lined graphite die of a sintering machine, which resided in an argon box to keep the integrity of the compound. Then, the powder was sintered together, meaning it was heated to high temperatures, but below melting points, until the powder adhered together in a uniform fashion. Finally, x-ray diffraction was used to confirm the final product as Yb_4LiGe_4, and energy dispersive x-ray spectroscopy was used to confirm its purity (negligible amounts of elemental germanium).[8]

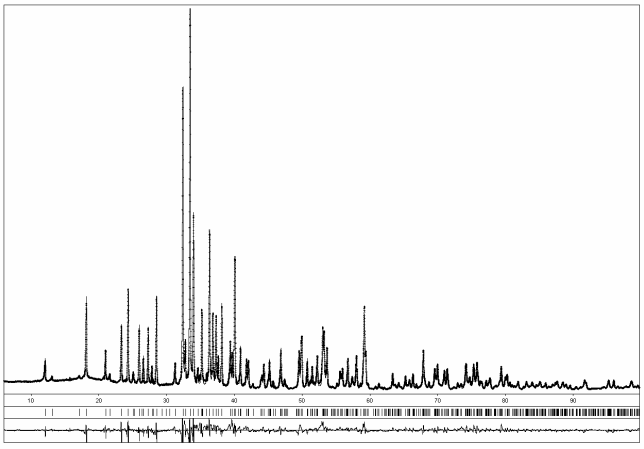

Figure 37: X-Ray Spectroscopy Data for Yb_4LiGe_4.[8]

Appendix B: Sample Preparation

To prepare the sample for the investigation of the pressure dependence on its magnetic properties, first a piece of Yb_4LiGe_4 was chosen because of its size and mostly rectangular shape. Then, the sample was cut down to a smaller size using a diamond saw. Subsequently, four brass wires were connected to the sample using silver epoxy with the orientation shown in Figure 30. Since the compound is moisture sensitive, the sample was kept in nitrogen gas when not being cut or having epoxy applied to it. The epoxy was allowed to dry overnight at room temperature in a nitrogen atmosphere. Then, the sample with wires was stored in nitrogen gas until it was time to mount it to the pressure cell.

Appendix C: Assembling the Pressure Cell

(This section of the thesis is written so that the procedure can be followed by the reader.)

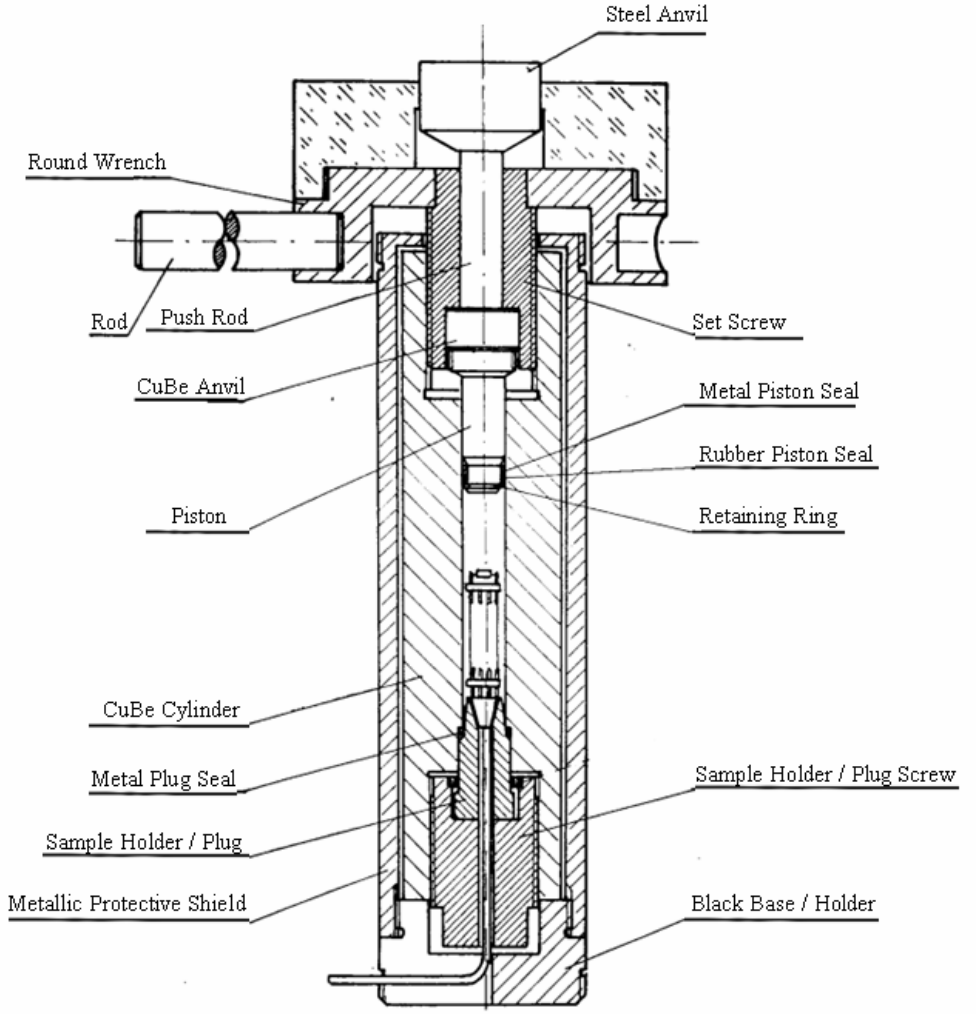

Figure 38: Diagram of Pressure Cell.[24]

First of all, the sample must be mounted onto the plug. Cut out a piece of cigarette paper with dimensions that are slightly larger than the sample. Then, apply a tiny dab of GE Varnish to the cigarette paper, and place the sample on the paper. Then, secure the sample with the cigarette paper to the plug with an additional tiny dab of Varnish in the orientation given by Figure 30 onto the sample holder / plug. Now, solder the wires to the proper contact posts of the plug. Check the electrical connections.

Next, remove any old seals and make sure the neck of the plug is cleaned with methanol before fitting a new metal seal from the bag labeled “Plug Seals” over the neck of the plug down to its base. Clean the copper – beryllium cylinder with methanol. Note that the end of the cylinder with numbers on it is the top. Secure the cylinder in a vice with the top pointing to the ground. Then, carefully insert the plug into the bottom of the cylinder, being sure not to hit the sides of the inside of the cylinder with the sample holder. Screw in the plug with a wrench. Then, use a torque wrench. Set the torque wrench so that it exerts a torque of about 10 N-m, and screw in the plug further (the torque wrench “clicks” once the torque applied is 10 N-m). Then, increase the torque slightly, and screw in the plug further. Keep increasing the torque in small increments until 28 N-m of torque has been applied to the plug. No more torque is needed after 28 N-m.

Remove the cell from the vice and put it in one of the black bases/holders so that the top of the cylinder points up. Check the electrical connections. Now, remove the horseshoe shaped piece of metal called the retaining ring without losing it. The best way to do this is to hold the bend of the horseshoe to the table with the piston, then apply pressure to one end of the horseshoe with a screwdriver while pulling the piston toward oneself. Again, do not lose this piece. Remove any old seals from the piston. Clean the piston and the copper-beryllium anvil with methanol. Fit a metal seal from the bag labeled “Metal Piston Seals” over the smaller part of the piston and push it down as far as it will go. Then, fit a rubber seal from the bag labeled “Rubber Piston Seals” over the piston, down to the metal seal. The rubber seal seals the piston in for low pressures, while the metal one is a good seal for higher pressures. Keep the seals in place by putting the retaining ring back on.

Now it is time to add Fluorinert, the pressure transmitting medium. The Fluorinert can be found under the fume hood. The type of Fluorinert is FC-77, which is a good pressure transmitting medium up to at least 9.5 kbar of applied pressure.[25] Use a plastic bulb syringe or eye dropper to slowly dispense Fluorinert into the inside of the cylinder where the sample is located. The fluid must be added slowly because air easily diffuses into it, which may cause air bubbles when pressure is applied. Fill the inner chamber to the top. Then, leave the pressure cell in the fume hood for several hours in order for air to diffuse out. Some of the fluid will evaporate. The ideal level for the Fluorinert is about 1-2 mm below the top of the inner chamber. A good amount of Fluorinert is tricky to get. Too much will lead to the piston pushing out the fluid and not sealing properly, but too little may lead to a plugged pressure cell. It may be necessary at this point to add a bit more fluid. Do so drop by drop, very slowly. If needed, remove some of the fluid by sucking it out with the bulb syringe.

Once a good level of Fluorinert is obtained, use the piston puller to carefully lower the piston straight down into the fluid. Remove the tool from the piston. Push down gently on the piston, and it should move down and resist like a small spring. Then, place the CuBe anvil on top of, and aligned with, the piston. Put the set screw directly over the piston and anvil so that the alignment is not altered. It is important that the piston is able to move directly down into the cell without hitting the walls. Screw the set screw down. Before too many turns, there should be strong resistance.

Appendix D: Pressurizing the Pressure Cell

Place the metallic protective shield over the cylinder and screw it into the black base. Next, put a little grease on the push rod and insert it into the hole of the set screw. Now, fit the round wrench onto the top of the cell, and place the steel anvil into the wrench.

Place the pressure cell in the center of the oil press (Laboratory Hydraulic Press: LCP20). Close the polycarbonate protective shields. Then, close the valve located at the bottom of the press by turning it clockwise. Pump on the press to raise the cell 3-4 mm. Screw the upper screw of the press down by turning the handle at the top of the press clockwise (from above) until the pressure cell is secured firmly. Pump slowly until the voltage display shows a value of about 1 V. Now, turn the round wrench clockwise (from above) by inserting the rod into one of the holes in the wrench and pushing to the left. The wrench should turn smoothly and easily with little resistance. If this is not the case, do not try to force the wrench to turn. This may result in jamming the cell, so the cell should be disassembled and reassembled.

After several turns, there will be resistance to further turning. When this occurs, pump on the press about 0.15 V, and then turn the wrench more. This time, the wrench should only turn about a quarter of the way before there is resistance again. At this point, the voltage will start to drop, which is normal. Then pump and turn the wrench again. Note that the voltage will jump up to the previous value very quickly, and then increase past that value at little slower. The pressure should be increased by about 0.15 V each time until the desired voltage is reached. This is the voltage that is displayed after pumping but before turning the wrench. To determine the desired voltage, use the voltage-to-resistance table, which is next to the press.

Throughout this process, the press has been lifting up the pressure cell. The pushing rod stays stationary but moves deeper inside the pressure cell from the pressure cell's frame of reference. This applies pressure to the piston, which applies pressure to the Fluorinert, which applies pressure to the sample. Turning the wrench screws the set screw down so that the piston stays put when the pushing rod is removed.

After reaching the desired pressure (voltage), open the valve at the bottom of the press. Once the voltage reading drops to zero, turn the handle at the top of the press to pull the upper screw away from the cell. Then, check the electrical connections.

Pressure Determination

The resistance from the pressure transducer can be converted into kbar with the following equations:

$$P(kbar) = 10 \cdot \left[\frac{-0.35228 + \sqrt{(0.35228)^2 - 4(0.0659)\left(1 - \frac{R(m\Omega)}{18.15 m\Omega}\right)}}{2(0.0659)} \right]$$

This equation is for use at room temperature. When the sample is cooled to 4.2 K, the following equation should be used:

$$P(kbar) = \left[2.73 + 6.434 \cdot 10^{-4} \cdot (T - 77.4K)\right] \cdot \ln\left[\frac{R(m\Omega, T)}{15.086 m\Omega}\right] \qquad \text{(At T = 4.2 K)}$$

Appendix E: Depressurizing the Pressure Cell

In order to decrease the pressure in the cell, the cell must be depressurized completely and disassembled that new seals can be used. Start by putting the cell in the oil press with all of its protective gear as it is described in the section about pressurizing the cell. Then, turn the valve to the right, and pump on the press to raise the cell a few millimeters. Lower the upper screw until is about 2 mm above the pressure cell. If the upper screw is not touching the pressure cell, the cell will not be able to depressurize. Now, pump on the press slowly until it reaches the voltage value corresponding to the pressure within the cell. Insert the rod into the wrench and turn the wrench counter-clockwise one full turn. Then, turn the valve to the left to relieve the pressure.

Once the voltage goes to zero, raise the upper screw and position it a couple of millimeters above the pressure cell. Pump on the oil press until the voltage reaches a value slightly below the previous value. Once pumping on the press becomes less effective, it is okay to stop at that value. Then, turn the wrench counter-clockwise one full turn, and turn the valve to the left to relieve the pressure.

Repeat the steps in the previous paragraph until the voltage goes below 1 V. At his point, the pushing rod should not be visible because the set screw will cover it. Then, raise the upper screw and remove the pressure cell from the press. Remove all of the protective equipment and the pushing rod from the pressure cell.

Now, use a wrench to unscrew the set screw completely, and then remove it. Take out the CuBe anvil, and use the piston puller to pull out the piston. Tthen pour out the Fluorinert into a waste container. Turn the pressure cell over, and use a wrench to unscrew the sample holder. Carefully remove the sample holder without hitting the sample or its connections

against the inside of the cylinder. Take off all of the seals, and store them in the bag of used seals in the wooden box on the lab counter. Now the pressure cell is disassembled.

Appendix F: Diagram of Dilution Refrigerator

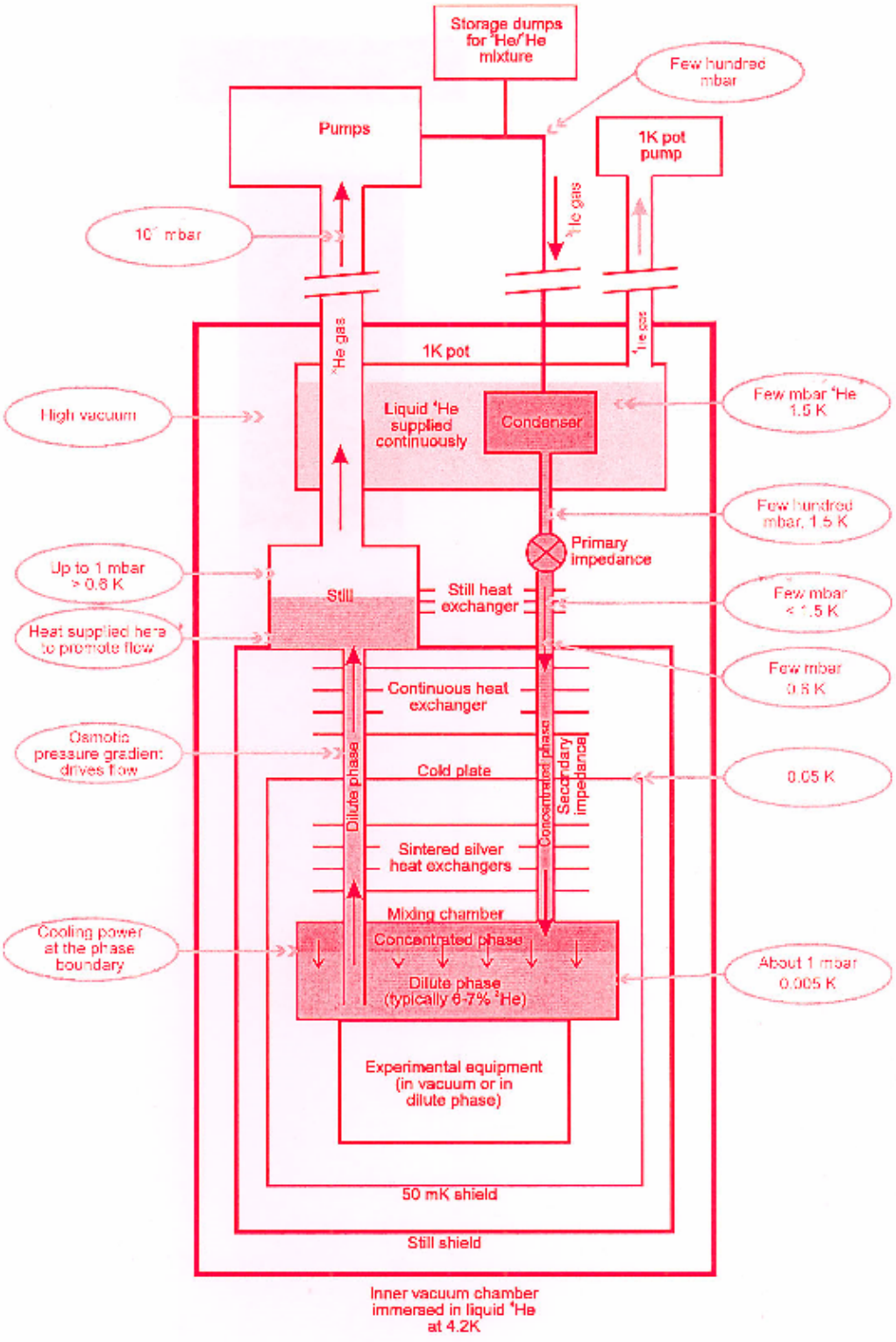

Figure 39: Diagram of Dilution Refrigerator.[22]

Appendix G: References

1. Griffiths, David. 1999. *Introduction to Electrodynamics*. New Jersey: Prentice-Hall, Inc.
2. Kittel, Charles. 2005. *Introduction to Solid State Physics*. New York: John Wiley & Sons, Inc.
3. Bertotti, Giorgio. 1998. *Hysteresis in Magnetism: For Physicists, Materials Scientists, and Engineers*. Massachusetts: Academic Press, Inc.
4. Wolf, W.P. 1961. Ferrimagnetism. *Rep. Prog. Phys.* 24: 212-303.
5. Pecharsky, V.K. and K.A. Gschneider, Jr. 2007. Structure, magnetism, and thermodynamics of the novel rare earth-based R_5T_4 intermetallics. *Pure Appl. Chem.* Vol. 79 No. 8: 1383-1402.
6. McGregor, Steve. 2007. Giant magnetocaloric materials could have large impact on the environment. *Argonne National Laboratory*. http://www.anl.gov/Media_Center/News/2007/news070618.html (accessed May 6, 2010).
7. Voyer, C.J. et al. 2006. Valence and magnetic ordering in the $Yb_5Si_xGe_{4-x}$ pseudobinary system. *Physical Review B* 73: 174422.
8. Sebastian, P. et al. 2010. Crystal Chemistry and Physical Properties of the Mixed Valent Rare-Earth Lithium Germanide Yb_4LiGe_4. Unpublished manuscript.
9. Lawrence, J.M. et al. 1981. Valence fluctuation phenomena. *Rep. Prog. Phys.* 44: 1-84.
10. Ahn, Kyunghan, et al. 2005. Phase relationships and structural, magnetic, and thermodynamic properties of the Yb_5Si_4-Yb_5Ge_4 pseudobinary system. *Physical Review B* 72: 054404.

11. Tobash, P.H. and Svilen Bobev. 2006. Structure and Bonding in Yb4MgGe4: Yb^{2+}/Yb^{3+} Mixed-Valency and Charge Separation. *J. Am. Chem. Soc.* 128: 3532 – 3533.

12. Graf, Michael. Address. Boston College. Chestnut Hill, MA, 2010.

13. Graf, Michael. 2010. *NMR Studies of Yb_4LiGe_4: A Possible Kondo Insulator* [PowerPoint slides].

14. Adams, Dean. 2006. *The ISIS Synchrotron* [PowerPoint slides].

15. Lord, J.S. *Muon Beam Lines* [PowerPoint slides]. Retrieved from ISIS Rutherford Appleton Laboratory website: www.isis.rl.ac.uk/

16. Graf, Michael. 2010. *The Lives and Deaths of Muons: Probing Magnetism in Condensed Matter Systems* [PowerPoint slides].

17. Garwin, Richard L. et al. 1957. Observations of the Failure of Conservation of Parity and Charge Conjugation in Meson Decays: The Magnetic Moment of the Free Muon. *Physical Review* 105(4).

18. Dalmas de Réotier, P. and A Yaouanc. 1997. Muon spin rotation and relaxation in magnetic materials. *J. Phys.: Condensed Matter* 9: 9113-9166.

19. Blundell, S.J. 2008. Spin-polarized muons in condensed matter physics. Retrieved from ISIS Rutherford Appleton Laboratory website: www.isis.rl.ac.uk/

20. Hillier, AD, et al. 2005. The MuSR User Guide. Retrieved from ISIS Rutherford Appleton Laboratory website: www.isis.rl.ac.uk/

21. USGS National Geomagnetism Program. http://geomag.usgs.gov/charts/

22. Oxford Instruments. 2007. *Operator's Handbook.*

23. Bauer, E. et al. 1997. Onset of magnetic order in $YbCu_{5-x}Al_x$. *Physical Review B* Vol. 56 No. 2: 711-718.

24. High Pressure Research Center, Polish Academy of Sciences. 2002. *LC10 Liquid Pressure Cell ID 7 MM*.

25. Varga, Tamas, et al. 2003. Fluorinert as a pressure-transmitting medium for high-pressure diffraction studies. *Review of Scientific Instruments* Vol 74, No. 10: 4565-4566.